of the microplates at a dilution of 1:200 in phosphate-buffered saline (PBS) containing 0.1% (w/v) bovine serum albumin (BSA) (fraction V, fatty acid-free: Merck KGaA, Darmstadt, Germany), 0.5% (v/v) Tween 20 and a mock protein [optical density (OD) at 280 nm = 0.5] obtained from the pupae of silkworms infected with a nonrecombinant baculovirus. As enzyme-labeled antibodies, a peroxidase-conjugated goat IgG fraction to rat IgG (whole molecule: MP Biomedicals, LLC., Solon, OH) was used for the rat anti-HEV IgG assay. The OD of each sample was read at 450 nm. The cutoff value was provisionally set at 0.234 as the mean plus five standard deviations (SDs) of the negative controls ($n = 366$); the details are described elsewhere. Test samples with OD values equal to or greater than the cutoff value were considered to be positive for anti-HEV IgG.

The specificity of the rat anti-HEV IgG assay was verified according to the level of absorption with the same recombinant rat HEV ORF2 protein (50 μg/ml at the final concentration) that was used as the antigen probe. Briefly, prior to testing, the serum samples were diluted 1:200–1:2000 to adjust the OD value to <1.5. If the OD value of the tested sample was reduced by ≥70% after absorption with the recombinant ORF2 protein, the sample was considered to be positive for anti-HEV.

2.4. Qualitative and quantitative detection of rat HEV RNA

Total RNA was extracted from 100 μl of each serum sample using the TRIzol LS Reagent (Life Technologies, Carlsbad, CA) according to the manufacturer's instructions. The RNA preparation thus obtained was reverse transcribed with SuperScript II RNase H^- reverse transcriptase (Life Technologies) and an antisense primer, HE663 [5′-CGC GGG CAA TCT CGC CA-3′ (nt 362–378)] specific for the rat HEV 5′-terminal sequence, then subjected to nested PCR in the presence of *TaKaRa Ex Taq* (TaKaRa Bio, Shiga, Japan); the nucleotides were numbered in accordance with the prototype rat HEV strain [R63 (GU345042)], unless otherwise stated. A portion of the 5′-terminal region sequence was amplified using the primer pair HE658 [sense: 5′-GCT ACC GCC TTT GCT AAT GC-3′ (nt 83–102)] and HE663 in the first round and HE660 [sense: 5′-CGC CTT TGC TAA TGC TCA GG-3′ (nt 88–107)] and HE659 [antisense: 5′-GCA ATC TCG CCA RCG YTG C-3′ (R = A or G; Y = T or C) (nt 355–373)] in the second round. The PCR amplification was performed for 35 cycles in the first round [94 °C for 30 s (with an additional 2 min in the first cycle); 55 °C for 30 s; 72 °C for 60 s (with an additional 7 min in the last cycle)] and 25 cycles in the second round, under the same conditions. The size of the amplification product of the first-round PCR was 296 base pairs (bp) and that of the second-round PCR was 286 bp. The PCR product of the second-round PCR was subjected to electrophoresis on agarose gel, and samples with a visible band of 286 bp were considered to be positive for rat HEV RNA.

The sequences of the above-mentioned primers were chosen from well-conserved regions of the entire rat HEV genome by comparing all reported rat HEV strains (GU345042, GU345043, JN167537, JN167538 and JX120573) in addition to the ratIDE079 and ratIDE113 strains whose entire genomic sequences were determined in the present study, using the previously described viremic serum samples (Mulyanto et al., 2013).

To confirm the presence of rat HEV RNA, a portion of the ORF1 and ORF2 junctional region (primarily the ORF1 region) was amplified via nested RT-PCR using the primer sets HE607 (sense) and H604 (antisense) in the first round and HE608 (sense) and HE606 (antisense) in the second round (ORF1-PCR), as previously described (Mulyanto et al., 2013); these sets generated amplification products of 899 bp (nt 4098–4996) and 880 bp (nt 4103–4982), respectively. The RT-PCR assay was performed in duplicate, and its reproducibility was confirmed. The specificity of the RT-PCR assay was verified using a sequence analysis, as described below.

The RNA of rat HEV was quantitated using real-time RT-PCR according to a previously described method (Tanaka et al., 2007) with slight modifications, employing an in vitro-transcribed rat HEV RNA as a standard. In brief, using the T7 BlueT vector containing a 341-nt fragment of ratIDE079 cDNA (nt 35–375) as a template and the AmpliScribe™ T7-*Flash*™ Transcription Kit (Epicentre Biotechnologies, Madison, WI), rat HEV RNA was transcribed in vitro, purified and used as a standard of rat HEV RNA. Total RNA was extracted from 10 to 100 μl of the serum samples using TRIzol-LS and subjected to real-time RT-PCR with a QuantiTect Probe RT-PCR Kit (Qiagen, Tokyo, Japan) using the sense primer HE655 [5′-CCA CGG GGG TTA ATA CTG C-3′ (nt 36–54)], the antisense primer HE656 [5′-CGG ATG CGA CCA AGA AAC AG-3′ (nt 189–208)] and a probe (HE657-P) consisting of an oligonucleotide with a 5′-reporter dye (6-carboxyfluorescein, FAM) and a 3′-quencher dye (6-carboxytetramethyl-rhodamine, TAMRA) [5′-FAM-CGG CTA CCG CCT TTG CTA ATG C-TAMRA-3′ (nt 81–102)] on an Applied Biosystems 7900HT Fast Real-Time PCR System (Applied Biosystems, Tokyo, Japan). The thermal cycler conditions were 50 °C for 30 min during stage 1, 95 °C for 15 min during stage 2, and 50 cycles of 94 °C for 15 s and 56 °C for 30 s during stage 3. The reproducibility of the quantitative assay was assessed by testing each sample in duplicate, and the mean value was adopted.

To prevent contamination during the procedures, the guidelines provided by Kwok and Higuchi (1989) were strictly followed.

2.5. Amplification of the full-length rat HEV genome

Total RNA was extracted from 200 μl of each of five serum samples and subjected to cDNA synthesis followed by nested PCR of three overlapping regions (301–336 nt, 1495–1824 nt and 2265–2805 nt) in the central portion of the HEV genome, excluding the extreme 5′- and 3′-terminal regions, using enzymes [KOD-plus (Toyobo, Osaka, Japan), *TaKaRa LA Taq* with GC Buffer (TaKaRa Bio) or *TaKaRa Ex Taq* (TaKaRa Bio)] and primers whose sequences were derived from well-conserved areas across all rat HEV strains (GU345042, GU345043, JN167537, JN167538 and JX120573) whose entire genomic sequences are known as well as those obtained during the amplification procedure. The extreme 5′-end sequence (nt 1–94 or 1–102) was determined using a modified rapid amplification of cDNA ends (RACE) technique called RNA ligase-mediated RACE (RLM-RACE) with the First Choice RLM-RACE Kit (Ambion, Austin, TX), as previously described (Okamoto et al., 2001). Amplification of the 3′-terminal region sequence (2825–2827 nt), excluding the poly(A) tail, was accomplished using the RACE technique, according to the previously described method (Okamoto et al., 2001).

2.6. Sequence analysis of the PCR products

The amplification products were purified using a FastGene Gel/PCR Extraction Kit (NIPPON Genetics Co. Ltd., Tokyo, Japan), after which both strands were directly sequenced using an Applied Biosystems 3130xl Genetic Analyzer (Life Technologies) with a BigDye Terminator v3.1 Cycle Sequencing Kit (Life Technologies). For the partial sequence analysis, the amplification products of ORF1-PCR (840 nt: the primer sequences at both ends were excluded) were determined. For the full-length sequence analysis, the extreme 5′-end sequence was determined based on the consensus sequence of at least five clones that were obtained after being inserted into the T-Vector, pMD20 (TaKaRa Bio), and the sequences of the remaining four overlapping regions, including the 3′-terminal region, of the rat HEV genome were determined directly. The sequence analysis was performed using the Genetyx software program (version 11.1.2; Genetyx Corp., Tokyo, Japan), and multiple alignments were generated with the CLUSTAL W

Table 1
Prevalence of anti-HEV IgG and HEV RNA in wild rats from Lombok and Central Java (Solo), Indonesia.

Region (Island/city or district)	No. of samples tested	Body weight (mean ± SD g)	Rat anti-HEV IgG	Rat HEV RNA	
				5′ terminus-PCR	ORF1-PCR
Lombok					
Mataram	216	111.4 ± 49.2	101 (46.8%)	54 (25.0%)	54 (25.0%)
West Lombok	17	91.6 ± 38.7	2 (11.8%)	2 (11.8%)	2 (11.8%)
Subtotal	233	110.0 ± 48.8	103 (44.2%)	56 (24.0%)	56 (24.0%)
Java (Central Java)					
Solo	136	83.6 ± 42.8	34 (25.0%)	43 (31.6%)	41 (30.6%)
Total	369	100.3 ± 48.3	137 (37.1%)	99 (26.8%)	97 (26.3%)

software program, version 2.1 (Thompson et al., 1994). Phylogenetic trees were constructed according to the neighbor-joining method (Saitou and Nei, 1987) with the Kimura two-parameter correction model and 1000 replicates of bootstrap resampling, as implemented in the MEGA 5 software program (version 5.2.1) (Tamura et al., 2011). The full-length nucleotide sequences of five rat HEV isolates (see Fig. 4 for the accession nos.) and the ORF2 region sequences (281 nt) of 26 rat HEV isolates (see Fig. 5 for the accession nos.) that were retrievable from the DDBJ/GenBank/EMBL databases as of August 2013 were included for comparison.

3. Results

3.1. Prevalence of anti-HEV antibodies and HEV RNA among wild rats

When the serum samples obtained from 233 wild rats on Lombok Island, Indonesia, were tested for the presence of rat anti-HEV IgG antibodies using ELISA, with a recombinant rat HEV ORF2 protein as an antigen probe, 101 (46.8%) of 216 samples obtained from the capital city of Lombok, Mataram had OD values that were equal to or greater than the provisional cutoff value (0.234; see Section 2) and were considered to be positive for rat anti-HEV IgG, while two (11.8%) of 17 samples obtained from West Lombok had detectable rat HEV antibodies (Table 1). All 136 serum samples obtained from wild rats captured in Solo, a city in Central Java, Indonesia, were also tested for the presence of rat anti-HEV IgG, and 34 (25.0%) samples were found to be positive. When the prevalence of HEV infection in the rats studied was stratified by weight as a measure of age, the rats showed an increasing tendency in the prevalence of anti-HEV IgG with weight in both Lombok and Solo (Table 2). The prevalence of HEV viremia was highest (29.2%) in the 101–150 g weight group in Lombok, while it was highest (60.0%) in the ≥151 g weight group, followed by the 101–150 g weight group (44.4%) in Solo.

All 369 samples were subjected to the detection of rat HEV RNA using RT-PCR with nested primers targeting the 5′-terminal region (5′-terminus-PCR), and 99 samples, including 56 samples (24.0%) obtained from Lombok and 43 samples (31.6%) obtained from Solo were found to have detectable rat HEV RNA. To confirm the positivity/negativity of rat HEV RNA, all rat serum samples were tested for the presence of rat HEV RNA using another nested RT-PCR analysis, ORF1-PCR, to amplify the ORF1-ORF2 junctional region (mostly the 3′-terminal ORF1 region). Consequently, all 56 5′-terminus-PCR-positive samples obtained from Lombok and 41 of the 43 5′-terminus-PCR-positive samples obtained from Solo were also found to be positive for rat HEV RNA detectable on ORF1-PCR. Two discrepant samples were repeatedly positive for rat HEV RNA on the 5′-terminus-PCR and undetectable on ORF1-PCR or real-time RT-PCR, suggesting that these two samples had a low viral load and that 5′-terminus-PCR is more sensitive than the ORF1-PCR, at least in the assay of Indonesian viremic samples.

Overall, 37.1% and 26.8% of the tested samples had detectable rat anti-HEV IgG and rat HEV RNA, respectively, and 67 samples (18.2%) were positive for both rat HEV antibodies and RNA.

3.2. Genetic heterogeneity of rat HEV strains in Indonesia

Since the ORF1-ORF2 region sequence amplified by ORF1-PCR was more variable and longer than 5′-terminal sequence amplified by 5′-terminus-PCR, the amplification products of ORF1-PCR (840 nt; the primer sequences at both ends were excluded) in all 97 viremic rats were sequenced directly, and their nucleotide sequences were compared. The 97 HEV strains were 76.3–100 (87.1 ± 7.6)% identical to each other within the 840-nt sequence and shared nucleotide sequence identities of 75.4–84.5 (77.5 ± 1.3)%, 75.6–84.1 (77.6 ± 1.1)%, 77.2–85.5 (79.2 ± 1.1)%, 76.6–85.5 (78.1 ± 1.2)% and 78.3–88.4 (84.3 ± 2.9)%, respectively, with the reported rat HEV sequences (GU345042, GU345043, JN167537, JN167538 and JX120573) whose entire genomic sequences are known. In contrast, the rat HEV strains obtained in the present study were only 57.6–64.0 (60.5 ± 1.0)% identical to representative human HEV strains of genotypes 1–4 [B1 (M73218), US1 (AF060668), MEX-14 (M74506) and T1 (AJ272108)] and only 51.5–70.3 (58.9 ± 7.0)% identical to ferret (JN998606), bat (JQ001749) and avian (AY535004) HEV strains. These results suggest that all 97 Indonesian rat HEV strains obtained from wild rat sera in the present study are most closely related to reported rat HEV strains, not to other mammalian or avian HEV strains.

A phylogenetic tree was constructed according to the neighbor-joining method based on the 840-nt ORF1 sequences of all 97 rat HEV strains obtained in the present study, 17 rat HEV strains from Indonesia obtained in our previous study (Mulyanto et al., 2013) and German and Vietnamese rat HEV strains (GU345042, GU345043, JN167537, JN167538 and JX120573) (Fig. 2) using a

Table 2
Prevalence of anti-HEV IgG and HEV RNA in wild rats stratified by weight as measure of age.

Weight (g)	Lombok (Mataram and West Lombok)			Java (Solo)		
	No. of samples tested	Rat anti-HEV IgG	Rat HEV RNA (5′ terminus-PCR)	No. of samples tested	Rat anti-HEV IgG	Rat HEV RNA (5′ terminus-PCR)
≤50	27	4 (14.8%)	2 (7.4%)	34	5 (14.7%)	9 (26.5%)
51–100	80	28 (35.0%)	19 (23.8%)	70	17 (24.3%)	19 (27.1%)
101–150	72	34 (47.2%)	21 (29.2%)	27	9 (33.3%)	12 (44.4%)
≥151	54	37 (68.5%)	14 (25.9%)	5	3 (60.0%)	3 (60.0%)
Total	233	103 (44.2%)	56 (24.0%)	136	34 (25.0%)	43 (31.6%)

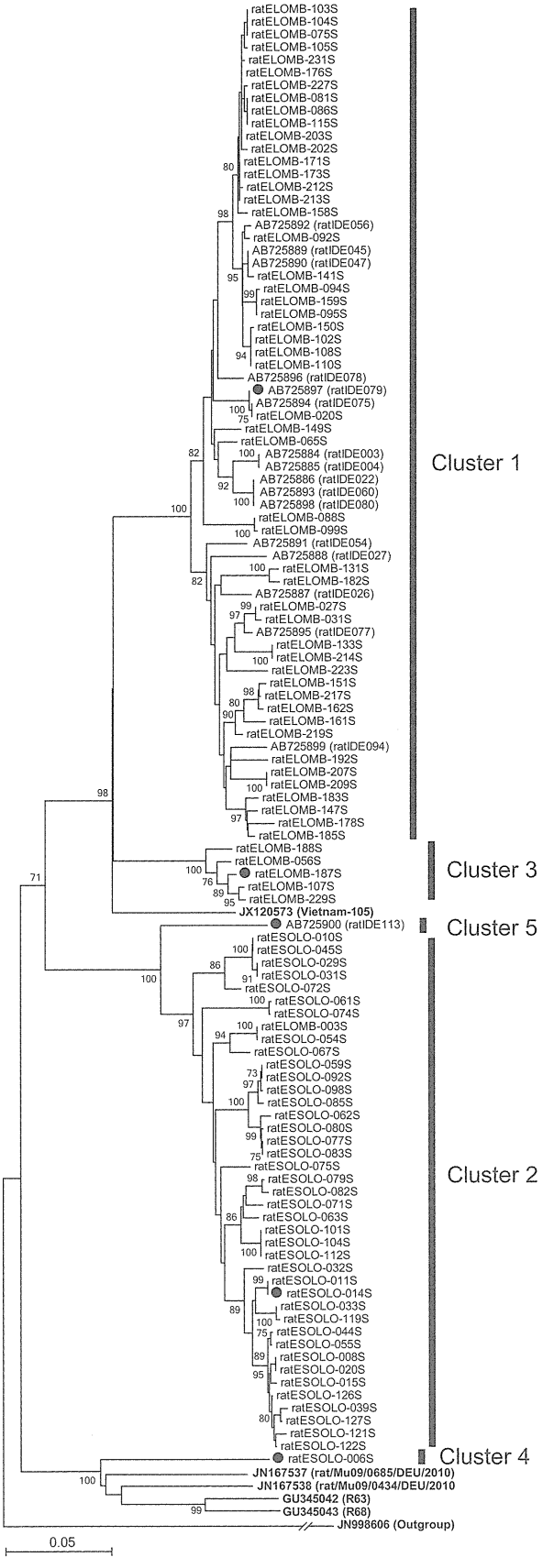

Fig. 2. Phylogenetic tree constructed according to the neighbor-joining method based on the 840-nucleotide ORF1-ORF2 partial sequences of 119 rat HEV strains, using ferret HEV (JN998606) as the outgroup. In addition to the 97 rat HEV strains obtained in the present study, 17 Indonesian rat HEV strains obtained in a previous study (Mulyanto et al., 2013) and five reported rat HEV strains obtained from Germany (GU345042, GU345043, JN167537 and JN167538) (Johne et al., 2010a, 2012) and Vietnam (JX120573) whose entire genomic sequences are known, as indicated with the strain name in parenthesis and in bold for visual clarity, were included for comparison. The five Indonesian rat HEV strains whose entire genomic sequences were determined in the present study are indicated by closed circles. The five phylogenetic clusters, provisionally designated in this study are highlighted by vertical bars. The bootstrap values (≥70%) are presented as the percentage of data obtained from 1000 resampling analyses. The scale bar indicates the number of nucleotide substitutions per site.

Table 3
Region-dependent distribution of rat HEV clusters and cluster-dependent HEV RNA titers.

Region/rat HEV cluster[a]	No. of samples compared	Rat HEV RNA titer [Log (copies/ml)]	
		Mean ± SD	Highest
Lombok			
Cluster 1	50	3.92 ± 1.39	5.51
Cluster 2	1	2.48	
Cluster 3	5	4.11 ± 0.41	4.61
Solo			
Cluster 2	40	2.73 ± 1.55	5.63
Cluster 4	1	2.48	

[a] See Fig. 2.

ferret HEV strain (JN998606) as an outgroup. The phylogenetic tree showed that the Indonesian rat HEV strains obtained in the present and previous studies form five phylogenetic clusters (tentatively designated as Clusters 1–5), comprising 66 isolates in Cluster 1, 41 isolates in Cluster 2, five isolates in Cluster 3 and one isolate each in Clusters 4 and 5, with the high bootstrap values of 100% for Cluster 1, 97% for Cluster 2 and 100% for Cluster 3. In support of this provisional classification, the mean identity% in the 840-nt ORF1-ORF2 sequence was 95.0–97.8% within clusters (Clusters 1–3) and 77.1–89.5% between clusters (Supplementary Table 1).

See Supplementary Table 1 as supplementary file. Supplementary material related to this article can be found, in the online version, at http://dx.doi.org/10.1016/j.virusres.2013.10.029.

Of note, 97 isolates obtained from Solo and Lombok in the present study were classified into four Clusters (1–4) and 17 isolates obtained from Lombok in our previous study (Mulyanto et al., 2013) were grouped into Cluster 1 ($n = 16$) or Cluster 5 ($n = 1$). These results indicate that polyphyletic strains of rat HEV are circulating in Indonesia: Cluster 1 strains were predominant on Lombok Island, while Cluster 2 strains were prevalent in Solo. Interestingly, a single Cluster 2 strain (ratELOMB-003S) was isolated in Lombok, with a nucleotide sequence identity of 93.9–99.7% to 40 strains belonging to the same cluster in Solo. As indicated in Table 3, a high HEV load was noted in the predominant strains represented by the Cluster 1 strains in Lombok, with a highest load of 3.2×10^5 copies/ml, and by the Cluster 2 strains in Solo, with a highest load of 4.3×10^5 copies/ml.

3.3. *Analysis of the full-length genomes of five rat HEV strains representing each of the five phylogenetic clusters (Clusters 1–5) in Indonesia*

The entire genomic sequence was determined for five Indonesian rat HEV strains (ratIDE079F, ratESOLO-014SF, ratELOMB-187SF, ratESOLO-006SF and ratIDE113F: highlighted with closed circles in Fig. 2), one from each of five clusters. These five rat HEV strains had a genomic length of 6928–6967 nt, excluding the poly(A) tract at the 3′-terminus, similar to the reported German and Vietnamese strains (GU345042, GU345043, JN167537, JN167538 and JX120573: 6940–6958 nt). The differences in genomic length were attributed to the deletion or insertion of nucleotides in the hypervariable region of ORF1 and 3′-UTR (Fig. 3A). The five strains

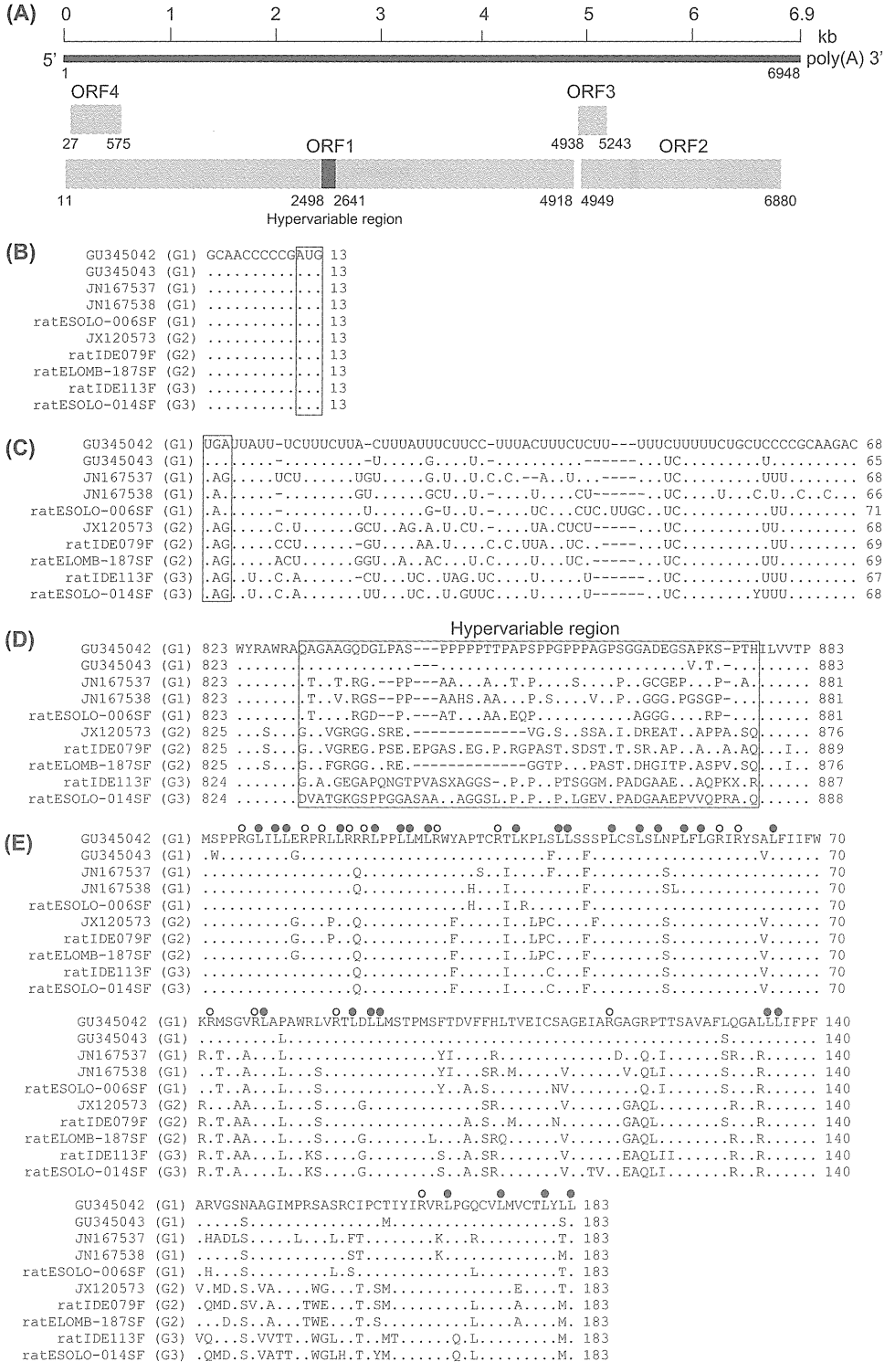

Fig. 3. (A) Organization of the rat HEV genome showing the location of ORF1 with a hypervariable region (illustrated by a closed box), ORF2, ORF3 and putative ORF4, indicated by gray bars. The nucleotide positions are in accordance with the prototype rat HEV strain (GU345042). (B) Comparison of the nucleotide sequences of the rat HEV strains containing the 5′-UTR and initiation codon (AUG) for ORF1. (C) Comparison of the nucleotide sequences of the rat HEV strains containing the 3′-UTR and termination codon (UGA, UAG or UAA) for ORF2. (D) Comparison of the amino acid sequences of the rat HEV strains within the indicated region of ORF1. The hypervariable region is boxed. (E) Comparison of the amino acid sequences of the rat HEV strains in the putative ORF4. Conserved arginine residues are indicated by open circles and conserved leucine residues are indicated by closed circles. Deletions are indicated by hyphens, and nucleotides (or amino acids) that are identical to those at the top are indicated by dots.

whose entire genomic sequences were determined in the present study possessed a common 5′-UTR sequence of GCAACCCCCG, identical to that of the reported German and Vietnamese strains (Fig. 3B), while the 3′-UTR of these 10 strains was variable in length (62–68 nt) and sequence, differing by 6.8–33.8 (25.9 ± 6.3)% in each strain, although all of the strains were rich in U, accounting for 56.1–66.2% of the total 3′-UTR sequence (Fig. 3C).

Each of the five strains obtained in the present study possessed three major ORFs, similar to reported mammalian and avian HEV strains (Meng et al., 2012; Tam et al., 1991). In each strain, ORF2 encoded 644 aa and ORF3 encoded 102 aa in common, while the length of ORF1 was variable (1629–1642 aa) due to a deletion/insertion in the hypervariable region, similar that observed in the reported German and Vietnamese strains (Fig. 3D). As for other putative ORFs found in the German strains (GU345042 and GU345043) (Johne et al., 2012), ORF4 with a coding capacity of 183 aa was commonly observed in all 10 rat HEV strains including the other two German strains as well as the Vietnamese and Indonesian strains, while ORF5 and ORF6 appear to be uncommon in rat HEV. Of note, the putative ORF4-encoded protein contained a relatively high proportion of leucine (17.5–19.1%) and arginine residues (10.4–12.6%); 27 leucine residues and 14 arginine residues were conserved among the 10 rat HEV strains (Fig. 3E).

The ratIDE079F, ratESOLO-014SF, ratELOMB-187SF, ratESOLO-006SF and ratIDE113F strains shared an identity of 76.6–91.2% over the entire genome. The ratESOLO-006SF strain was 86.4–86.7% identical to the reported German rat HEV strains (GU345042, GU345043, JN167537 and JN167538) over the entire genome, although it was only 76.8% identical to the Vietnamese strain (JX120573). The German strains and Vietnamese strain were provisionally classified into Genetic group 1 (G1) and G2, respectively, in the present study, and ratESOLO-006SF was tentatively grouped into G1 (Table 4). The ratIDE079S and ratELOMB-187SF strains shared 87.6% identity over the entire genome and were 86.8–88.3% identical to the Vietnamese strain (G2) and only 76.5–77.4% identical to the G1 strains, indicating that they can be classified into G2. The ratIDE113F and ratESOLO-014SF strains differed from each other by only 8.8% over the entire genome. However, they were only 76.4–77.6% identical to the G1 strains and only 80.2–80.9% similar to the G2 strains, suggesting the presence of a third new genetic group of rat HEV (G3). Therefore, the ratIDE113F and ratESOLO-014SF strains were considered to be members of a new genetic group (G3).

In order to further characterize the full-length sequences of the ratIDE079F, ratESOLO-014SF, ratELOMB-187SF, ratESOLO-006SF and ratIDE113F strains obtained in the present study, a phylogenetic tree was constructed based on the entire genomic sequences of 10 rat HEV strains, including the five strains obtained in the current study, two reported ferret strains and a bat HEV strain (JQ001749), as well as representative HEV strains of genotypes 1–4 and two wild boar HEV strains that may be classifiable into novel genotypes (Smith et al., 2013; Takahashi et al., 2010, 2011), using avian HEV strains of genotypes 1–3 as outgroups (Fig. 4). The tree showed that the ratIDE079F, ratESOLO-014SF, ratELOMB-187SF, ratESOLO-006SF and ratIDE113F strains can be grouped with the four German and one Vietnamese rat HEV strains, forming three separate groups (G1, G2 and G3) supported by high bootstrap values of 100% each.

3.4. Comparison with rat HEV strains whose partial sequences are known and the provisional classification of rat HEV strains

As indicated in Table 5, a comparison of the seven representative rat HEV strains whose entire genomic sequence is known, including the prototype German strain [GU345042 (G1)], Vietnamese strain [JX120573 (G2)] and five Indonesian strains of Clusters 1–5 (G1–G3) obtained in the present study, with reported partial rat HEV sequences of 216–4019 nt suggested that rat HEV strains in Germany, the United States and Denmark are closely related to GU345042 (G1) and thus can be grouped into G1. Among the rat HEV strains in three clusters (A–C) reported from China (Li et al., 2013c), the Cluster A strains were closest to JX120573 (G2), with

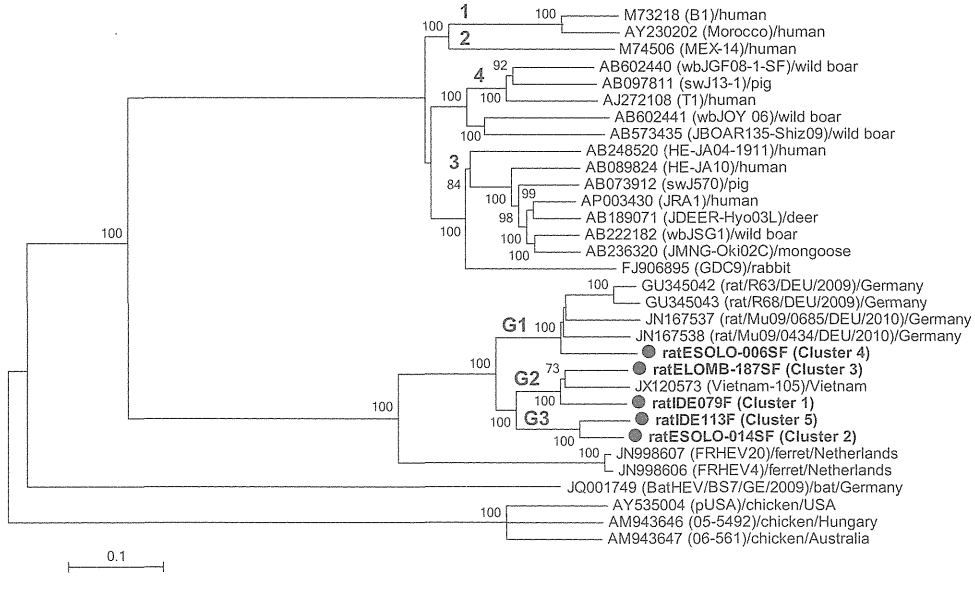

Fig. 4. Phylogenetic tree constructed according to the neighbor-joining method based on the entire genomic sequences of 29 HEV strains, using avian HEV strains of genotypes 1–3 (AY535004, AM943646 and AM943647) as the outgroups. In addition to the five rat HEV strains whose entire genomic sequences were determined in the present study, as highlighted by closed circles, five reported rat HEV strains from Germany (GU345042, GU345043, JN167537 and JN167538) and Vietnam (JX120573), representative HEV genotypes 1–4 strains, two HEV strains from wild boars that may be segregated into two distinct genotypes (AB573435 and AB602441) (Smith et al., 2013), two ferret HEV strains (JN998606 and JN998607) and a bat HEV strain (JQ001749) were included for comparison. Each reported HEV strain is presented with the accession no., the name of the strain in parenthesis and the animal species from which it was isolated (for HEV genotype 1–4 strains and the two wild boar HEV strains) or the country in which it was isolated (for the rat, ferret, bat and avian HEV strains). G1, G2 and G3 represent Genetic groups 1, 2 and 3, respectively, that were provisionally designated in the present study. The bootstrap values (≥70%) are indicated as the percentage of data obtained from 1000 resampling analyses. The scale bar indicates the number of nucleotide substitutions per site.

Table 4
Sequence homology between rat HEV isolates allowing for three-category classification.

Rat HEV strain[a]	Percentage identity to full-length nucleotide (ORF1 amino acid) sequence of[b]:						
	GU345042 (G1)	ratESOLO-006SF (Cluster 4/G1)	JX120573 (G2)	ratIDE079F (Cluster 1/G2)	ratELOMB-187SF (Cluster 3/G2)	ratIDE113F (Cluster 5/G3)	ratESOLO-014SF (Cluster 2/G3)
GU345042	–	**86.5 (95.0)**	76.9 (87.0)	76.8 (87.3)	76.8 (87.1)	76.4 (86.4)	76.9 (87.1)
GU345043	**95.2 (97.7)**	**86.7 (94.6)**	76.8 (86.5)	76.7 (86.6)	76.6 (86.6)	76.9 (85.9)	77.1 (86.7)
JN167537	**86.7 (94.6)**	**86.4 (96.0)**	76.9 (87.4)	77.4 (87.5)	77.3 (87.7)	76.7 (86.6)	77.6 (87.6)
JN167538	**87.1 (94.6)**	**86.7 (95.5)**	77.3 (87.9)	77.4 (87.3)	77.4 (87.6)	77.0 (86.8)	77.5 (88.0)
ratESOLO-006SF	**86.5 (95.0)**	–	76.8 (87.9)	77.4 (87.7)	76.5 (87.8)	76.6 (87.0)	77.0 (87.7)
JX120573	76.9 (87.0)	76.8 (87.9)	–	**86.8 (94.7)**	**88.3 (95.8)**	80.9 (90.9)	80.4 (91.1)
ratIDE079F	76.8 (87.3)	77.4 (87.7)	**86.8 (94.7)**	–	**87.6 (94.8)**	80.5 (90.8)	80.2 (91.1)
ratELOMB-187SF	76.8 (87.1)	76.5 (87.8)	**88.3 (95.8)**	**87.6 (94.8)**	–	80.2 (90.3)	80.2 (90.8)
ratIDE113F	76.4 (86.4)	76.6 (87.0)	80.9 (90.9)	80.5 (90.8)	80.2 (90.3)	–	**91.2 (96.3)**
ratESOLO-014SF	76.9 (87.1)	77.0 (87.7)	80.4 (91.1)	80.2 (91.1)	80.5 (90.8)	**91.2 (96.3)**	–

[a] See Fig. 4 for the reference for each rat HEV strain.
[b] Highest identity scores (≥86.4% at the nucleotide level and ≥94.6% at the amino acid level) are in bold.

Table 5
Comparison of seven representative rat HEV strains, including five strains whose entire genomic sequences were determined in the present study, with the reported partial rat HEV sequences.

Rat HEV isolates	No. of isolates compared	Length of nucleotide compared	Nucleotide identity (%) with[a]:						
			GU345042 (G1)	ratESOLO-006SF (Cluster 4/G1)	JX120573 (G2)	ratIDE079F (Cluster 1/G2)	ratELOMB-187SF (Cluster 3/G2)	ratIDE113F (Cluster 5/G3)	ratESOLO-014SF (Cluster 2/G3)
Germany	9	216–4019	84.2–**95.8**	83.7–86.6	76.3–81.9	75.3–82.0	76.3–79.1	76.7–78.6	76.4–78.7
USA	1	327	**87.7**	84.3	85.9	79.7	80.6	80.0	81.9
Denmark	1	282	**84.8**	80.4	78.7	79.7	78.2	79.2	81.3
China	17	281	75.9–81.0	76.7–81.3	80.6–93.5	78.2–89.9	78.9–91.4	79.8–85.6	82.3–87.8
Cluster A	8	281	77.4–80.7	76.7–80.2	87.8–**93.5**	84.6–89.9	87.8–91.4	84.1–85.6	84.5–87.8
Cluster B	3	281	75.9–79.3	77.8–78.5	84.5–**85.6**	83.5–83.9	84.2–**85.6**	81.7–83.8	84.5–85.3
Cluster C	6	281	79.2–81.0	80.6–81.3	80.6–82.0	78.2–80.4	78.9–81.1	79.8–80.9	82.3–**83.0**
Indonesia	109	840	75.4–79.6	76.3–79.0	80.4–88.4	79.1–99.8	79.6–98.5	79.1–91.1	78.6–99.8
Cluster 1	65	840	77.1–79.6	77.1–79.0	85.2–87.8	91.5–**99.8**	85.4–88.5	79.1–82.0	78.6–80.7
Cluster 2	40	840	75.4–77.1	76.3–77.9	80.4–82.2	79.1–80.4	79.6–81.5	89.5–91.1	94.6–**99.8**
Cluster 3	4	840	78.0–78.4	78.4–78.9	88.2–88.4	87.0–87.8	97.3–**98.5**	80.9–81.5	81.0–81.3

[a] Highest identity scores are in bold.

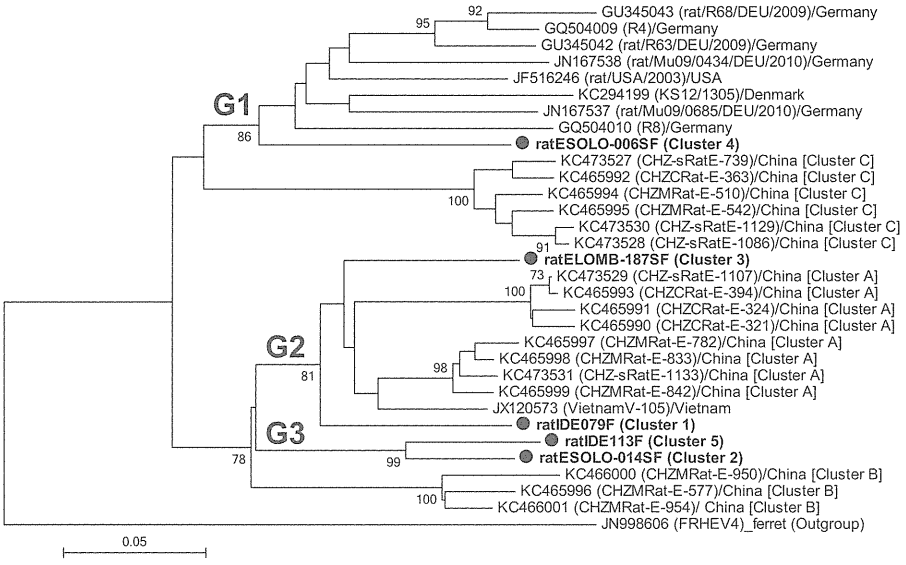

Fig. 5. Neighbor-joining tree of the 281 nt sequence alignment within ORF2 containing 31 rat HEV strains and the outgroup strain. In addition to five reported rat HEV strains from Germany and Vietnam with known entire genomic sequences and five Indonesian rat HEV strains whose entire genomic sequences were determined in the present study, as highlighted by closed circles, 21 reported rat HEV strains from Germany (Johne et al., 2012), the United States (Purcell et al., 2011), Denmark (Wolf et al., 2013) and China (Li et al., 2013c) whose common 281-nt ORF2 sequence is available were included for comparison. Each reported rat HEV strain is presented with the accession no., the name of the strain in parenthesis and the country in which it was isolated. G1–G3 represent Genetic groups 1–3, respectively, that were provisionally designated in the present study. The bootstrap values (≥70%) are indicated as a percentage of the data obtained from 1000 resampling analyses. The scale bar indicates the number of nucleotide substitutions per site.

a highest nucleotide sequence identity of 93.5%, thus suggesting that the Chinese Cluster A strains are classifiable into G2. On the other hand, Cluster B strains exhibited a highest nucleotide sequence identity of only 85.6% with JX120573 (G2) and ratELOMB-187SF (G2), and the Cluster C strains showed a highest nucleotide sequence identity of only 83.0% with ratESOLO-014SF (G3).

A plylogenetic tree based on the common 281-nt sequence indicated that the US and European strains including those from Germany and Denmark, can be grouped into G1, with a bootstrap value of 89% and Chinese Cluster A strains segregate into G2, with a bootstrap value of 81% (Fig. 5). The Chinese Cluster B and Cluster C strains were located separately from the G1–G3 branches, suggesting the presence of two additional genetic groups.

4. Discussion

The present study revealed that wild rats on both Lombok Island and in Central Java (Solo) of Indonesia are frequently infected with rat HEV and that polyphyletic strains of rat HEV provisionally classifiable into five phylogenetic clusters (Clusters 1–5) differing from each other by 10.5–22.9% within the 840-nt ORF1-ORF2 sequence are circulating in wild rats in Indonesia. When 17 rat HEV strains obtained from Lombok in our previous study [Cluster 1 ($n = 16$) and Cluster 5 ($n = 1$)] (Mulyanto et al., 2013) were included, a total of 73 rat HEV strains in Lombok were segregated into Cluster 1 ($n = 66$), Cluster 2 ($n = 1$), Cluster 3 ($n = 5$) and Cluster 5 ($n = 1$), while 41 rat HEV strains in Central Java were separated into Clusters 2 ($n = 40$) and 4 ($n = 1$). These results suggest the geographical clustering of Clusters 1 and 3–5, excluding Cluster 2. A further analysis of the entire genomic sequences of five Indonesian rat HEV strains representing one of each of the five phylogenetic clusters demonstrated that the Indonesian rat HEV strains can be segregated into three distinct genetic groups [a German type (Cluster 4), Vietnamese type (Clusters 1 and 3) and novel type (Clusters 2 and 5)] differing from each other by 19.5–23.5 (22.0 ± 1.7)% over the entire genome, suggesting the circulation of rat HEV strains belonging to all thus far recognized three genetic groups in Indonesia.

The high prevalence of rat anti-HEV IgG and rat HEV viremia noted among wild rats on Lombok Island in the present study confirmed the frequent infection with rat HEV observed in wild rats on the same island in our previous study (Mulyanto et al., 2013). The detection of rat HEV in wild rats from the same villages, including Kr. Kelok and Kr. Kemong in Mataram city and Labuapi in West Lombok on Lombok Island, at different time points additionally suggests the continuing presence of the virus in the local rat population (Supplementary Table 2), likely due to lower sanitary conditions and high densities of the human and rat populations. In the present study, frequent infection was also noted among wild rats in Solo, a city in Central Java, where wild rats are commonly captured by residents in their houses, suggesting a wide distribution of the virus in wild rats in Indonesia. Surprisingly, a rat HEV strain (ratESOLO-006SF) belonging to G1 was identified in the Mangkunegara village of Solo city. This finding may be explained by the historical relationship between Mangkunegara and European countries. Around the middle of the 18th century, the Dutch intensively occupied Solo Kingdom, including Mangkunegara. The occupation lasted until Indonesia obtained its independence in 1945. Hence, it is tempting to speculate that the G1 rat HEV strain was imported from a European country in the past, most likely the Netherlands. To date, the palaces of Solo Kingdom and Mangkunegara still exist, and the area surrounding Mangkunegara Palace is called Mangkunegara Village.

See Supplementary Table 2 as supplementary file. Supplementary material related to this article can be found, in the online version, at http://dx.doi.org/10.1016/j.virusres.2013.10.029.

By determining the full-length genomic sequences of five Indonesian rat HEV strains in the present study, a total of 10 entire genomic sequences of rat HEV have been made available, including four German strains (GU345042, GU345043, JN167537 and JN167538) and a Vietnamese strain (JX120573), which enables the comparison of genetic heterogeneity among the strains in conserved and divergent regions. The phylogenetic analysis of complete HEV genomes confirmed that rat HEV is related distantly to mammalian HEV and segregated to a distant branch, as previously indicated by Johne et al. (2010a, 2012). Moreover, the results clearly demonstrated that rat HEV can be divided into

three different genetic groups (Fig. 3), i.e., a German type (G1), including the four reported German strains and an Indonesian strain (ratESOLO-006SF) derived from Solo, a Vietnamese type (G2), including JX120573 and the two Indonesian strains, ratIDE079F and ratELOMB-187SF, derived from Lombok and a novel or presumably Indonesia indigenous type (G3) represented by two Indonesian strains (ratIDE113F and ratESOLO-014SF) derived from Lombok and Solo, respectively. The intragroup difference was 4.8–13.6% among G1 strains, 11.7–13.2% among G2 strains and 8.8% among G3 strains over the entire genome, while the intergroup difference was 22.6–23.4% between the G1 and G2 strains, 22.4–23.6% between the G1 and G3 strains and 19.1–19.8% between the G2 and G3 strains (Table 4), thus indicating a clear separation into three genetic groups, further supported by high bootstrap values of 100% (Fig. 3). Avian HEV strains obtained from chickens are separated into three different genotypes (1: Australia, 2: United States and 3: Europe) based on an inter-genotype difference of 17.1–18.0% over the near-entire genome sequence (Bilic et al., 2009). In addition, it has been proposed that the Vietnamese rat HEV strain is a new member of the rat HEV genotype. These descriptions support the division of rat HEV strains into three different "genotypes" [genotype 1 for German, US, Denmark and Indonesian (Cluster 4) strains; genotype 2 for Vietnamese and Indonesian (Clusters 1 and 3) strains; and genotype 3 for Indonesian (Clusters 2 and 5) and Chinese (Cluster A) strains (Table 5 and Fig. 4). However, for rat HEV, no generally accepted threshold has been defined thus far to distinguish between genotypes. A pairwise comparison of HEV genotypes 1–4 from humans, pigs, wild boars, deer and mongooses over the entire genome revealed an inter-genotype difference of 23.6–27.7% (Okamoto, 2007). Although only 281-nt sequences have been determined, the phylogenetic tree depicted in Fig. 4 suggests the presence of additional genetic groups containing Chinese rat HEV strains of Clusters B and C. Furthermore, the designation "genotype" has a specific meaning in HEV terminology (e.g., human HEV genotypes 1–4). A unified system of nomenclature for the HEV genotypes/subgenotypes should be determined based on comparative analyses of complete genome sequences in accordance with many precedents, such as that used for the hepatitis C virus (Simmonds et al., 2005) and hepatitis B virus (Kramvis et al., 2008; Okamoto et al., 1988). Until the complete genomic sequences of additional rat HEV strains, including those present in thus far unexamined areas, have been accumulated and a distinct definition of a rat HEV genotype is identified, another designation "genetic group" or "lineage" should be used for novel rat HEV strains, and continued efforts to accumulate sequence data for complete HEV genomes that may be classifiable into novel genotypes are needed in future studies.

Although 66 rat HEV strains (Cluster 1) and five Cluster 3 strains from Lombok were classified as belonging to the Vietnamese type (G2), they differed from the Vietnamese strain (JX120573) by 12.2–14.8% and 11.6–11.8%, respectively, suggesting the indigenousness of rat HEV strains (G2: Clusters 1 and 3) in Indonesia. Likewise, a Cluster 5 strain in Lombok and 40 Cluster 2 strains in Solo shared nucleotide sequence identities of only 89.5–91.1%, suggesting the geographical clustering of G3 rat HEV strains in Indonesia. This phenomenon may occur in this country due to its shape as an archipelago.

The nucleotide sequences of rat HEV strains presented in this study exhibit a high degree of variation in the rat HEV genome. Sequence divergence is not evenly distributed over the entire genome. The 5′-UTR of rat HEV is unique in that it has only a 10-nt sequence of GCAACCCCCG in common, similar to that observed in ferret HEV (GGCAGACCCCTA) (Raj et al., 2012), although clearly different from that noted in other mammalian HEVs (25 nt for human HEV genotypes 1–4 and two wild boar strains, with a putative stem and loop structure, and 33 nt for bat HEV) and avian HEV (24 nt) (Huang et al., 2004). In contrast, the 3′-UTR of rat HEV is variable in both length and sequence. The length of ORF1, except for the hypervariable region, and the lengths of ORF2 and ORF3 are well conserved among all 10 rat HEV strains, similar to that seen in known HEV strains. Of note is that putative ORF4 capable of encoding 183 aa is present in all 10 rat HEV strains and is also found in the ferret HEV genomes (Raj et al., 2012). Although the putative ORF4-encoded protein is characterized by an abundance of leucine and arginine in both the rat and ferret HEV strains, a BLASTp homology search of amino acid sequences deposited in the DDBJ/EMBL/GenBank databases indicated only very low sequence similarities with known proteins. Of note, a bat HEV strain possesses an ORF corresponding to ORF4 in the rat and ferret HEV genomes, encoding 219 aa rich in leucine (13.2%) and serine (11.4%). Further investigations are needed to elucidate the expression and functional roles of the putative ORF4-encoded protein.

Recently, genotype 3 HEV strains have been genetically detected from wild rats in the United States, suggesting the potential for zoonotic transmission and the genetic variability of rat HEV (Lack et al., 2012), although HEV strains (genotypes 1–4) were not detectable in wild rats in Indonesia in our previous study (Mulyanto et al., 2013). Since, under experimental conditions, laboratory rats are not susceptible to experimental infection by HEV strains (genotypes 1–3) (Li et al., 2013a; Purcell et al., 2011), further studies are warranted to independently confirm the existence of genotype 3 HEV in rats.

In conclusion, the present study revealed that polyphyletic rat HEV strains are frequently found in wild rats living in both Central Java and Lombok in Indonesia and that Indonesian rat HEV strains are segregated into three distinct genetic groups (a German type, Vietnamese type and novel type) that differ from each other by 19.5–23.5 (22.0 ± 1.7)% over the entire genome, thus suggesting a wide distribution of rat HEV with a markedly divergent genomic sequence. The wide range of rat HEV sequence variation reflects the nature of this pathogen as an RNA virus, as typified by influenza A and human immunodeficiency viruses (Steinhauer and Holland, 1987). Obviously, additional rat HEV isolates must be sequenced in order to fully characterize the range of variations in this virus. Like all RNA viruses, HEV is known to exist as a mixture of heterogeneous viruses defining quasispecies (Grandadam et al., 2004; Lhomme et al., 2012). Since sequence data determined in the present study were single in each individual, further investigations focused on quasispecies nature of rat HEV in each individual or in each genetic cluster are needed in future studies. The knowledge gathered will shed light on the global distribution of various rat HEV groups, and help to establish the route of transmission that maintains rat HEV in the population.

Acknowledgements

This study was supported in part by grants from the Ministry of Health, Labor and Welfare of Japan and from the Ministry of Education, Culture, Sports, Science and Technology of Japan.

References

Batts, W., Yun, S., Hedrick, R., Winton, J., 2011. A novel member of the family Hepeviridae from cutthroat trout (*Oncorhynchus clarkii*). Virus Res. 158 (1/2), 116–123.

Bilic, I., Jaskulska, B., Basic, A., Morrow, C.J., Hess, M., 2009. Sequence analysis and comparison of avian hepatitis E viruses from Australia and Europe indicate the existence of different genotypes. J. Gen. Virol. 90 (Pt 4), 863–873.

Colson, P., Borentain, P., Queyriaux, B., Kaba, M., Moal, V., Gallian, P., Heyries, L., Raoult, D., Gerolami, R., 2010. Pig liver sausage as a source of hepatitis E virus transmission to humans. J. Infect. Dis. 202 (6), 825–834.

Dalton, H.R., Bendall, R., Ijaz, S., Banks, M., 2008. Hepatitis E: an emerging infection in developed countries. Lancet Infect. Dis. 8 (11), 698–709.

Drexler, J.F., Seelen, A., Corman, V.M., Fumie Tateno, A., Cottontail, V., Melim Zerbinati, R., Gloza-Rausch, F., Klose, S.M., Adu-Sarkodie, Y., Oppong, S.K., Kalko,

E.K., Osterman, A., Rasche, A., Adam, A., Muller, M.A., Ulrich, R.G., Leroy, E.M., Lukashev, A.N., Drosten, C., 2012. Bats worldwide carry hepatitis E virus-related viruses that form a putative novel genus within the family Hepeviridae. J. Virol. 86 (17), 9134–9147.

Emerson, S.U., Nguyen, H.T., Torian, U., Burke, D., Engle, R., Purcell, R.H., 2010. Release of genotype 1 hepatitis E virus from cultured hepatoma and polarized intestinal cells depends on open reading frame 3 protein and requires an intact PXXP motif. J. Virol. 84 (18), 9059–9069.

Emerson, S.U., Purcell, R.H., 2013. Hepatitis E virus. In: Knipe, D.M., Howley, P.M., Cohen, J.I., Griffin, D.E., Lamb, R.A., Martin, M.A., Racaniello, V.R., Roizman, B. (Eds.), Fields Virology, 2 vols, sixth ed. Lippincott Williams & Wilkins, Philadelphia, pp. 2242–2258.

Graff, J., Torian, U., Nguyen, H., Emerson, S.U., 2006. A bicistronic subgenomic mRNA encodes both the ORF2 and ORF3 proteins of hepatitis E virus. J. Virol. 80 (12), 5919–5926.

Graff, J., Zhou, Y.H., Torian, U., Nguyen, H., St Claire, M., Yu, C., Purcell, R.H., Emerson, S.U., 2008. Mutations within potential glycosylation sites in the capsid protein of hepatitis E virus prevent the formation of infectious virus particles. J. Virol. 82 (3), 1185–1194.

Grandadam, M., Tebbal, S., Caron, M., Siriwardana, M., Larouze, B., Koeck, J.L., Buisson, Y., Enouf, V., Nicand, E., 2004. Evidence for hepatitis E virus quasispecies. J. Gen. Virol. 85 (Pt 11), 3189–3194.

Hoofnagle, J.H., Nelson, K.E., Purcell, R.H., 2012. Hepatitis E. N. Engl. J. Med. 367 (13), 1237–1244.

Huang, F.F., Sun, Z.F., Emerson, S.U., Purcell, R.H., Shivaprasad, H.L., Pierson, F.W., Toth, T.E., Meng, X.J., 2004. Determination and analysis of the complete genomic sequence of avian hepatitis E virus (avian HEV) and attempts to infect rhesus monkeys with avian HEV. J. Gen. Virol. 85 (Pt 6), 1609–1618.

Izopet, J., Dubois, M., Bertagnoli, S., Lhomme, S., Marchandeau, S., Boucher, S., Kamar, N., Abravanel, F., Guerin, J.L., 2012. Hepatitis E virus strains in rabbits and evidence of a closely related strain in humans, France. Emerg. Infect. Dis. 18 (8), 1274–1281.

Johne, R., Dremsek, P., Kindler, E., Schielke, A., Plenge-Bonig, A., Gregersen, H., Wessels, U., Schmidt, K., Rietschel, W., Groschup, M.H., Guenther, S., Heckel, G., Ulrich, R.G., 2012. Rat hepatitis E virus: geographical clustering within Germany and serological detection in wild Norway rats (*Rattus norvegicus*). Infect. Genet. Evol. 12 (5), 947–956.

Johne, R., Heckel, G., Plenge-Bönig, A., Kindler, E., Maresch, C., Reetz, J., Schielke, A., Ulrich, R.G., 2010a. Novel hepatitis E virus genotype in Norway rats, Germany. Emerg. Infect. Dis. 16 (9), 1452–1455.

Johne, R., Plenge-Bonig, A., Hess, M., Ulrich, R.G., Reetz, J., Schielke, A., 2010b. Detection of a novel hepatitis E-like virus in faeces of wild rats using a nested broad-spectrum RT-PCR. J. Gen. Virol. 91 (Pt 3), 750–758.

Kamar, N., Bendall, R., Legrand-Abravanel, F., Xia, N.S., Ijaz, S., Izopet, J., Dalton, H.R., 2012. Hepatitis E. Lancet 379 (9835), 2477–2488.

Kamar, N., Rostaing, L., Izopet, J., 2013. Hepatitis e virus infection in immunosuppressed patients: natural history and therapy. Semin. Liver Dis. 33 (1), 62–70.

Kramvis, A., Arakawa, K., Yu, M.C., Nogueira, R., Stram, D.O., Kew, M.C., 2008. Relationship of serological subtype, basic core promoter and precore mutations to genotypes/subgenotypes of hepatitis B virus. J. Med. Virol. 80 (1), 27–46.

Kwok, S., Higuchi, R., 1989. Avoiding false positives with PCR. Nature 339 (6221), 237–238.

Lack, J.B., Volk, K., Van Den Bussche, R.A., 2012. Hepatitis E virus genotype 3 in wild rats, United States. Emerg. Infect. Dis. 18 (8), 1268–1273.

Lhomme, S., Abravanel, F., Dubois, M., Sandres-Saune, K., Rostaing, L., Kamar, N., Izopet, J., 2012. Hepatitis E virus quasispecies and the outcome of acute hepatitis E in solid-organ transplant patients. J. Virol. 86 (18), 10006–10014.

Li, T.C., Ami, Y., Suzaki, Y., Takeda, N., Takaji, W., 2013a. No evidence for hepatitis E virus genotype 3 susceptibility in rats. Emerg. Infect. Dis. 19 (8), 1343–1345.

Li, T.C., Ami, Y., Suzaki, Y., Yasuda, S.P., Yoshimatsu, K., Arikawa, J., Takeda, N., Takaji, W., 2013b. Characterization of full genome of rat hepatitis E virus strain from Vietnam. Emerg. Infect. Dis. 19 (1), 115–118.

Li, T.C., Chijiwa, K., Sera, N., Ishibashi, T., Etoh, Y., Shinohara, Y., Kurata, Y., Ishida, M., Sakamoto, S., Takeda, N., Miyamura, T., 2005. Hepatitis E virus transmission from wild boar meat. Emerg. Infect. Dis. 11 (12), 1958–1960.

Li, W., Guan, D., Su, J., Takeda, N., Wakita, T., Li, T.C., Ke, C.W., 2013c. High prevalence of rat hepatitis E virus in wild rats in China. Vet. Microbiol. 165 (3/4), 275–280.

Meng, X.J., 2010. Recent advances in Hepatitis E virus. J. Viral Hepat. 17 (3), 153–161.

Meng, X.J., 2011. From barnyard to food table: the omnipresence of hepatitis E virus and risk for zoonotic infection and food safety. Virus Res. 161 (1), 23–30.

Meng, X.J., Anderson, D., Arankalle, V.A., Emerson, S.U., Harrison, T.J., Jameel, S., Okamoto, H., 2012. Hepeviridae. In: King, A.M.Q., Adams, M.J., Carstens, E.B., Lefkowitz, E.J. (Eds.), Virus Taxonomy, Ninth Report of the International Committee on Taxonomy of Viruses. Elsevier/Academic Press, Oxford, pp. 1021–1028.

Mizuo, H., Suzuki, K., Takikawa, Y., Sugai, Y., Tokita, H., Akahane, Y., Itoh, K., Gotanda, Y., Takahashi, M., Nishizawa, T., Okamoto, H., 2002. Polyphyletic strains of hepatitis E virus are responsible for sporadic cases of acute hepatitis in Japan. J. Clin. Microbiol. 40 (9), 3209–3218.

Mulyanto, Depamede, S.N., Sriasih, M., Takahashi, M., Nagashima, S., Jirintai, S., Nishizawa, T., Okamoto, H., 2013. Frequent detection and characterization of hepatitis E virus variants in wild rats (*Rattus rattus*) in Indonesia. Arch. Virol. 158 (1), 87–96.

Nidaira, M., Takahashi, K., Ogura, G., Taira, K., Okano, S., Kudaka, J., Itokazu, K., Mishiro, S., Nakamura, M., 2012. Detection and phylogenetic analysis of hepatitis E viruses from mongooses in Okinawa, Japan. J. Vet. Med. Sci. 74 (12), 1665–1668.

Okamoto, H., 2007. Genetic variability and evolution of hepatitis E virus. Virus Res. 127 (2), 216–228.

Okamoto, H., Takahashi, M., Nishizawa, T., Fukai, K., Muramatsu, U., Yoshikawa, A., 2001. Analysis of the complete genome of indigenous swine hepatitis E virus isolated in Japan. Biochem. Biophys. Res. Commun. 289 (5), 929–936.

Okamoto, H., Tsuda, F., Sakugawa, H., Sastrosoewignjo, R.I., Imai, M., Miyakawa, Y., Mayumi, M., 1988. Typing hepatitis B virus by homology in nucleotide sequence: comparison of surface antigen subtypes. J. Gen. Virol. 69 (Pt 10), 2575–2583.

Pudupakam, R.S., Kenney, S.P., Córdoba, L., Huang, Y.W., Dryman, B.A., Leroith, T., Pierson, F.W., Meng, X.J., 2011. Mutational analysis of the hypervariable region of hepatitis e virus reveals its involvement in the efficiency of viral RNA replication. J. Virol. 85 (19), 10031–10040.

Purcell, R.H., Emerson, S.U., 2008. Hepatitis E: an emerging awareness of an old disease. J. Hepatol. 48 (3), 494–503.

Purcell, R.H., Engle, R.E., Rood, M.P., Kabrane-Lazizi, Y., Nguyen, H.T., Govindarajan, S., St Claire, M., Emerson, S.U., 2011. Hepatitis E virus in rats, Los Angeles, California, USA. Emerg. Infect. Dis. 17 (12), 2216–2222.

Raj, V.S., Smits, S.L., Pas, S.D., Provacia, L.B., Moorman-Roest, H., Osterhaus, A.D., Haagmans, B.L., 2012. Novel hepatitis E virus in ferrets, the Netherlands. Emerg. Infect. Dis. 18 (8), 1369–1370.

Saitou, N., Nei, M., 1987. The neighbor-joining method: a new method for reconstructing phylogenetic trees. Mol. Biol. Evol. 4 (4), 406–425.

Sato, Y., Sato, H., Naka, K., Furuya, S., Tsukiji, H., Kitagawa, K., Sonoda, Y., Usui, T., Sakamoto, H., Yoshino, S., Shimizu, Y., Takahashi, M., Nagashima, S., Jirintai Nishizawa, T., Okamoto, H., 2011. A nationwide survey of hepatitis E virus (HEV) infection in wild boars in Japan: identification of boar HEV strains of genotypes 3 and 4 and unrecognized genotypes. Arch. Virol. 156 (8), 1345–1358.

Simmonds, P., Bukh, J., Combet, C., Deleage, G., Enomoto, N., Feinstone, S., Halfon, P., Inchauspe, G., Kuiken, C., Maertens, G., Mizokami, M., Murphy, D.G., Okamoto, H., Pawlotsky, J.M., Penin, F.O., Sablon, E., Tadasu, S.I., Stuyver, L., Thiel, H.J., Viazov, S., Weiner, A., Widell, A., 2005. Consensus proposals for a unified system of nomenclature of hepatitis C virus genotypes. Hepatology 42 (4), 962–973.

Smith, D.B., Purdy, M.A., Simmonds, P., 2013. Genetic variability and the classification of hepatitis E virus. J. Virol. 87 (8), 4161–4169.

Steinhauer, D.A., Holland, J.J., 1987. Rapid evolution of RNA viruses. Annu. Rev. Microbiol. 41, 409–433.

Takahashi, K., Kitajima, N., Abe, N., Mishiro, S., 2004. Complete or near-complete nucleotide sequences of hepatitis E virus genome recovered from a wild boar, a deer, and four patients who ate the deer. Virology 330 (2), 501–505.

Takahashi, K., Terada, S., Kokuryu, H., Arai, M., Mishiro, S., 2010. A wild boar-derived hepatitis E virus isolate presumably representing so far unidentified genotype 5. Kanzo 51 (9), 536–538.

Takahashi, M., Nishizawa, T., Sato, H., Sato, Y., Jirintai Nagashima, S., Okamoto, H., 2011. Analysis of the full-length genome of a hepatitis E virus isolate obtained from a wild boar in Japan that is classifiable into a novel genotype. J. Gen. Virol. 92 (Pt 4), 902–908.

Takahashi, M., Nishizawa, T., Tanaka, T., Tsatsralt-Od, B., Inoue, J., Okamoto, H., 2005. Correlation between positivity for immunoglobulin A antibodies and viraemia of swine hepatitis E virus observed among farm pigs in Japan. J. Gen. Virol. 86 (Pt 6), 1807–1813.

Takahashi, M., Okamoto, H., 2013. Features of hepatitis E virus infection in humans and animals in Japan. Hepatol. Res., http://dx.doi.org/10.1111/hepr.12175.

Tam, A.W., Smith, M.M., Guerra, M.E., Huang, C.C., Bradley, D.W., Fry, K.E., Reyes, G.R., 1991. Hepatitis E virus (HEV): molecular cloning and sequencing of the full-length viral genome. Virology 185 (1), 120–131.

Tamura, K., Peterson, D., Peterson, N., Stecher, G., Nei, M., Kumar, S., 2011. MEGA5: molecular evolutionary genetics analysis using maximum likelihood, evolutionary distance, and maximum parsimony methods. Mol. Biol. Evol. 28 (10), 2731–2739.

Tanaka, T., Takahashi, M., Kusano, E., Okamoto, H., 2007. Development and evaluation of an efficient cell-culture system for Hepatitis E virus. J. Gen. Virol. 88 (Pt 3), 903–911.

Tei, S., Kitajima, N., Takahashi, K., Mishiro, S., 2003. Zoonotic transmission of hepatitis E virus from deer to human beings. Lancet 362 (9381), 371–373.

Thompson, J.D., Higgins, D.G., Gibson, T.J., 1994. CLUSTAL W: improving the sensitivity of progressive multiple sequence alignment through sequence weighting, position-specific gap penalties and weight matrix choice. Nucleic Acids Res. 22 (22), 4673–4680.

Wolf, S., Reetz, J., Johne, R., Heiberg, A.C., Petri, S., Kanig, H., Ulrich, R.G., 2013. The simultaneous occurrence of human norovirus and hepatitis E virus in a Norway rat (*Rattus norvegicus*). Arch. Virol. 158 (7), 1575–1578.

Yamada, K., Takahashi, M., Hoshino, Y., Takahashi, H., Ichiyama, K., Nagashima, S., Tanaka, T., Okamoto, H., 2009. ORF3 protein of hepatitis E virus is essential for virion release from infected cells. J. Gen. Virol. 90 (Pt 8), 1880–1891.

Yazaki, Y., Mizuo, H., Takahashi, M., Nishizawa, T., Sasaki, N., Gotanda, Y., Okamoto, H., 2003. Sporadic acute or fulminant hepatitis E in Hokkaido, Japan, may be food-borne, as suggested by the presence of hepatitis E virus in pig liver as food. J. Gen. Virol. 84 (Pt 9), 2351–2357.

Zhao, C., Ma, Z., Harrison, T.J., Feng, R., Zhang, C., Qiao, Z., Fan, J., Ma, H., Li, M., Song, A., Wang, Y., 2009. A novel genotype of hepatitis E virus prevalent among farmed rabbits in China. J. Med. Virol. 81 (8), 1371–1379.

Zhou, X., de Man, R.A., de Knegt, R.J., Metselaar, H.J., Peppelenbosch, M.P., Pan, Q., 2013. Epidemiology and management of chronic hepatitis E infection in solid organ transplantation: a comprehensive literature review. Rev. Med. Virol. 23 (5), 295–304.

Supplementary Table 1

Comparison of all 114 Indonesian rat HEV strains of Clusters 1–5 whose 840-nt ORF1-ORF2 sequence was determined in the present study (n = 97) or in the previous study (n = 17)

Intra- and inter-cluster comparison	Identity% (mean ± SD)
Within one cluster	
Cluster 1 (n = 66)	95.0 ± 2.3
Cluster 2 (n = 41)	95.7 ± 1.6
Cluster 3 (n = 5)	97.8 ± 0.9
Cluster 4 (n = 1)	-
Cluster 5 (n = 1)	-
Between different clusters	
Cluster 1 vs. Cluster 2	80.0 ± 0.5
Cluster 1 vs. Cluster 3	87.3 ± 0.8
Cluster 1 vs. Cluster 4	78.2 ± 0.5
Cluster 1 vs. Cluster 5	78.2 ± 0.5
Cluster 2 vs. Cluster 3	80.6 ± 0.6
Cluster 2 vs. Cluster 4	77.1 ± 0.4
Cluster 2 vs. Cluster 5	89.5 ± 0.5
Cluster 3 vs. Cluster 4	78.5 ± 0.3
Cluster 3 vs. Cluster 5	81.3 ± 0.2
Cluster 4 vs. Cluster 5	77.6

Supplementary Table 2

Prevalence of anti-HEV IgG and HEV RNA in wild rats from the same villages in Lombok, Indonesia in the previous and present studies

	Previous study (August 2011-February 2012)[a]			Present study (October 2012)		
	No. of samples tested	Rat anti-HEV IgG	Rat HEV RNA	No. of samples tested	Rat anti-HEV IgG	Rat HEV RNA
Mataram						
Babakan	8	1 (12.5%)	0	16	3 (18.8%)	1 (6.3%)
Cemara	9	0	0	12	2 (16.7%)	1 (8.3%)
Dasan Agung	2	0	0	20	4 (20.0%)	2 (10.0%)
Dasan Sari	3	0	0	13	1 (7.7%)	2 (10.0%)
Kr. Kelok	25	9 (36.0%)	8 (32.0%)	20	6 (30.0%)	2 (10.0%)
Kr. Kemong	17	3 (17.6%)	3 (17.6%)	119	77 (64.7%)	41 (34.5%)
Majeluk	2	1 (50.0%)	1 (50.0%)	3	0	0
Pagutan	4	0	1 (25.0%)	2	0	0
West Lombok						
Labuapi	18	2 (11.1%)	1 (5.6%)	11	2 (18.2%)	2 (18.2%)

[a]Retrieved from Mulyanto et al. (2013).

Arch Virol
DOI 10.1007/s00705-013-1912-3

ORIGINAL ARTICLE

The membrane on the surface of hepatitis E virus particles is derived from the intracellular membrane and contains trans-Golgi network protein 2

Shigeo Nagashima · Masaharu Takahashi · Suljid Jirintai · Tanggis · Tominari Kobayashi · Tsutomu Nishizawa · Hiroaki Okamoto

Received: 17 May 2013 / Accepted: 28 October 2013
© Springer-Verlag Wien 2013

Abstract Our previous studies demonstrated that hepatitis E virus (HEV) requires the multivesicular body (MVB) pathway to release virus particles, suggesting that HEV utilizes the cellular ESCRT machinery in the cytoplasm, not at the cell surface, to be released from infected cells. In this study, we generated a murine monoclonal antibody (mAb) against the membrane-associated HEV particles to examine whether the membrane is derived from intracellular vesicles or the cell surface. An established mAb, TA1708, was found to capture the membrane-associated HEV particles, but not the membrane-dissociated particles or fecal HEV, in an immunocapture RT-PCR assay. Furthermore, digitonin treatment confirmed that the membrane on the surface of cell-culture-generated HEV particles was a lipid membrane. Double immunofluorescence staining revealed that mAb TA1708 specifically recognizes trans-Golgi network protein 2 (TGOLN2), an intracellular antigen derived from the trans-Golgi network. Supporting these findings, HEV particles with lipid membranes and ORF3 proteins on their surface were found abundantly in the lysates of HEV-infected cells. These results indicate that HEV forms membrane-associated particles in the cytoplasm, most likely by budding into intracellular vesicles, and that the released HEV particles with a lipid membrane retain the antigenicity of TGOLN2 on their surface.

S. Nagashima · M. Takahashi · S. Jirintai · Tanggis · T. Kobayashi · T. Nishizawa · H. Okamoto (✉)
Division of Virology, Department of Infection and Immunity, Jichi Medical University School of Medicine, 3311-1 Yakushiji, Shimotsuke, Tochigi 329-0498, Japan
e-mail: hokamoto@jichi.ac.jp

Published online: 13 November 2013

Introduction

Hepatitis E virus (HEV), a member of the genus *Hepevirus* in the family *Hepeviridae*, is the causative agent of acute and fulminant hepatitis E, which occurs in many parts of the world, principally as a water-borne infection in developing countries and zoonotically in industrialized countries [5, 6, 9, 35, 43, 47]. HEV has a single-stranded, positive-sense RNA genome of approximately 7,200 nucleotides (nt). The genome is capped and polyadenylated [19, 40] and contains a 5' untranslated region (UTR), three open reading frames (ORFs; ORF1, ORF2 and ORF3), a 3′ UTR and a poly(A) tail at the 3′ terminus [11]. ORF1 encodes non-structural proteins, including methyltransferase, papain-like cysteine protease, helicase and RNA-dependent RNA polymerase [1, 21]. ORF2 and ORF3 overlap, and the ORF2 and ORF3 proteins are translated from a bicistronic subgenomic RNA of 2.2 kb in length [15, 17]. The ORF2 protein is the viral capsid protein, while the ORF3 protein is a small protein of only 113 or 114 amino acids (aa) that is suggested to act as an adapter to link the intracellular transduction pathways, reduce the host inflammatory response and protect virus-infected cells [5]. Recently, it was found that ORF3 proteins play an important role in virion egress from infected cells [12, 30, 45].

Four major genotypes (1-4) of HEV have been identified in humans. While HEV genotypes 1 and 2 have only been found in humans and are associated with epidemics in developing countries, HEV genotypes 3 and 4 are zoonotic and responsible for sporadic cases of disease worldwide [32]. A number of animal strains of HEV have also been identified in several animal species including chickens, pigs, wild boars, rabbits and rats [28].

HEV particles present in feces and bile are non-enveloped, while those in circulating blood and culture supernatant have been found to be covered with a cellular membrane, similar to

enveloped viruses [39]. Enveloped viruses acquire their envelope by budding through cellular membranes of different origin. HIV-1 becomes enveloped while budding through the plasma membrane, and the release of nascent virions requires a membrane fission event that separates the viral envelope from the cell surface [10]. To facilitate this crucial step in its life cycle, HIV-1 exploits the endosomal sorting complexes required for the transport (ESCRT) complexes (ESCRT-I, ESCRT-II and ESCRT-III) that constitute the cellular membrane remodeling and fission machinery known as the ESCRT pathway [14]. Other enveloped RNA viruses, such as the Ebola virus [26], avian sarcoma virus (ASV) [33] and, more recently, hepatitis C virus (HCV) [3, 7], have also been shown to utilize ESCRT complexes during virion morphogenesis. Furthermore, enveloped DNA viruses, including hepatitis B virus (HBV) [23] and herpes simplex virus 1 (HSV-1) [8], have been reported to exploit the multivesicular body (MVB) machinery.

In our previous study, we demonstrated that the PSAP motif(s) in the ORF3 protein is necessary for the egress of HEV particles from infected cells and proposed that the PSAP motifs in the ORF3 protein play a role as the functional domain required for virion release associated with lipids and the ORF3 protein [30]. Furthermore, tumor susceptibility gene 101 (Tsg101), a cellular factor involved in the budding of viruses containing the P(T/S)AP late domain and a component of ESCRT-I, and the enzymatic activity of vacuolar protein sorting-associated protein 4A (Vps4A) and VPs4B are involved in the release of HEV virions, thus suggesting that HEV utilizes the MVB machinery to exit cells [31]. However, the nature and origin of the virion membrane have not yet been characterized.

In this study, we generated a murine monoclonal antibody (mAb) against membrane-associated HEV particles using purified cell-culture-generated HEV particles as immunogens. An established mAb, TA1708, bound specifically to the component of the membrane on the surface of the HEV particles and reacted with an intracellular antigen that was found to be trans-Golgi network protein 2 (TGOLN2) in double staining immunofluorescence studies; however, it did not react with the plasma membrane. The membrane-associated HEV particles were present abundantly in lysates of infected cells. Based on the results obtained in the present study, we propose that HEV utilizes the endomembrane for membrane formation and budding and that TGOLN2 is a surface antigen of membrane-associated HEV particles.

Materials and methods

Cell culture

PLC/PRF/5 cells (ATCC no. CRL-8024) were grown in Dulbecco's modified Eagle's medium (DMEM) containing 10 % (vol/vol) heat-inactivated fetal calf serum (FCS), 100 U/ml of penicillin, 100 μg/ml of streptomycin and 2.5 μg/ml of amphotericin B (growth medium) at 37 °C in a humidified 5 % CO_2 atmosphere, as described previously [42].

Viruses

A fecal suspension containing a wild-type genotype 3 HEV (JE03-1760F strain; 2.0×10^7 copies/ml) [36] and a culture supernatant containing a cell-culture-generated JE03-1760F variant (1.2×10^8 copies/ml) [24] were used as reference viruses in this study. HEV progenies in the culture supernatant of PLC/PRF/5 cells transfected with RNA transcripts of an infectious HEV cDNA clone (pJE03-1760F/wt, GenBank accession no. AB437316) and its derivative ORF3-deficient mutant (pJE03-1760F/ΔORF3, GenBank accession no. AB437317), whose initiation codon of the ORF3 gene was mutated to GCA (Ala), were used for the experiments [46].

Preparation of membrane-associated HEV particles as immunogens

The cell-culture-adapted JE03-1760F strain in the 23rd generation of supernatant passage (JE03-1760F_p23) [24] was cultivated in PLC/PRF/5 cells in a 75-cm^2 culture bottle (Asahi Glass Co. Ltd., Tokyo, Japan) with growth medium for more than 120 days, and culture media (204 ml) harvested during days 34-102 were pooled. The pooled culture media were spun down in a Beckman SW28 rotor (Beckman Coulter, Inc., Indianapolis, IN) at 112,700 × g at 10 °C for 5 h. The resulting pellets were suspended in 2 ml of TEN buffer containing 0.01 M Tris-HCl (pH 7.5), 0.001 M EDTA and 0.1 NaCl and subjected to sucrose density gradient ultracentrifugation as described previously [38]. A 2-ml volume of pooled peak fractions at a sucrose density of 1.14 g/ml was used as a viral suspension for immunization.

Production of mAbs

mAbs were raised against purified cell-culture-generated HEV particles using a method described elsewhere [44], with slight modifications. Briefly, BALB/c mice were injected three times intraperitoneally with 100 or 150 μl of the viral suspension (1.3×10^{10} copies/ml) in PBS on days 0, 14 and 53 and with 0.1 μg of inactivated pertussis toxin (Pertussis Toxin Salt-Free; List Biological Laboratories, Inc., Campbell, CA) on day 161 as an adjuvant, followed by the intravenous injection of 75 μl of the same viral suspension (with the adjuvant) on day 192, three days before fusion. NS-1 myeloma cells were fused with

immunized spleen cells at a ratio of 1:10. The screening of mAbs was performed using immunocapture RT-PCR as described below. Hybridomas secreting mAbs against membrane-associated HEV particles of the desired specificity were propagated in the peritoneal cavities of mice that had been made ascitic due to the injection of 2,6,10,14-tetramethylpentadecane. The ascites fluid was harvested approximately 10 days after implantation, and the γ-globulin fractions were precipitated with 2 M $(NH_4)_2SO_4$ and then purified via gel filtration in Sephadex G-200 (GE Healthcare UK Ltd., Buckinghamshire, England). The mAbs were tested for their immunoglobulin class/subclass using a murine monoclonal antibody isotyping kit (Bio-Rad Laboratories, Hercules, CA).

Immunocapture RT-PCR assay

To screen mAbs with virus-binding ability, immunocapture RT-PCR was performed as described previously [38] with the following modifications. In brief, the wells of the immunoplate (part no. 762071; Greiner Bio-One GmbH, Frickenhausen, Germany) were washed with saline three times, and 50 μl each of 10 μg/ml goat affinity-purified antibody to murine IgG (#55479; MP Biomedicals, Santa Ana, CA) and mouse IgM (#55484; MP Biomedicals) in saline was added to each well and immobilized. The wells were incubated at room temperature overnight and then washed five times with saline. Fifty microliters of culture supernatant containing mAbs was added to each well and incubated with shaking at room temperature for 1.5 h. The solution in each well was removed, and the wells were washed three times with saline. Fifty microliters of diluted culture supernatant containing HEV progeny (approximately 10^5 copies/ml) was added to each well and incubated with shaking at room temperature for 2 h and then incubated with shaking at 4 °C overnight. The solution in each well was removed, and the wells were washed three times with saline. One hundred fifty microliters of TRIzol® LS Reagent (Invitrogen, Carlsbad, CA) and 50 μl of distilled water were directly added twice to each well. The RNA was then extracted and subjected to quantitative detection of HEV RNA as described below.

To evaluate the specificity of the established mAbs and further characterize the HEV particles, an immunocapture RT-PCR assay was also performed, with or without prior treatment of HEV particles with 0.1 % (vol/vol) sodium deoxycholate and/or 0.1 % (wt/vol) trypsin at 37 °C for 2 h, or 1.5 % (wt/vol) digitonin (Nacalai Teaque, Kyoto, Japan) at room temperature for 13 h. In addition to the mAb (TA1708) against membrane-associated HEV particles generated in the present study, an anti-ORF2 mAb (H6225) [37] and an anti-ORF3 mAb (TA0536) [38] were used.

Quantitation of HEV RNA

RNA extraction was performed using TRIzol® LS Reagent (Invitrogen). Quantification of HEV RNA was performed by real-time RT-PCR using a LightCycler apparatus (Roche Diagnostics, Mannheim, Germany), with a QuantiTect Probe RT-PCR Kit (QIAGEN, Hilden, Germany), primer set, and a probe targeting the ORF2 and ORF3 overlapping region, as described previously [37].

Digitonin treatment and sucrose density gradient centrifugation

The culture supernatants containing HEV progeny (1.0×10^6 copies), collected from PLC/PRF/5 cells transfected with RNA transcripts of pJE03-1760F/wt or pJE03-1760F/ΔORF3 at 18 days post-transfection, were treated with or without 1.5 % digitonin at room temperature for 13 h. The digitonin-treated culture supernatants were subjected to equilibrium centrifugation in a sucrose density gradient as described previously [38]. The gradients were fractionated, and the density of each fraction was measured using refractometry. Similarly, the culture supernatant containing 6.0×10^6 copies of HEV or cell lysates containing 5.0×10^7 copies of HEV collected from the PLC/PRF/5 cells transfected with RNA transcripts of pJE03-1760F/wt at 28 days post-transfection were subjected to equilibrium centrifugation in a sucrose density gradient.

Immunofluorescence assay

PLC/PRF/5 cells in a 4-well chamber slide (Nunc, Roskilde, Denmark) were subjected to immunofluorescence staining using mAb TA1708 and rabbit polyclonal antibodies raised against well-established cellular markers (see below) as the primary antibodies, followed by Alexa Fluor 488–conjugated anti-mouse IgM (Molecular Probes, Eugene, OR) and Alexa Fluor 594–conjugated anti-rabbit IgG (Molecular Probes) as the secondary antibodies. For staining of Myc-tagged TGOLN2 recombinant protein in the cells transfected with expression plasmid (see below), anti-Myc mAb (9E10; Santa Cruz Biotechnology) labeled by using a Zenon Alexa Fluor 488 mouse IgG labelling kit (Molecular Probes) as well as mAb TA1708 as the primary antibody and Alexa Fluor 568–conjugated anti-mouse IgM (Molecular Probes) as the secondary antibody, or anti-TGOLN2 antibody (HPA012723; Sigma-Aldrich, St Louis, Mo) as the primary antibody and Alexa Fluor 594–conjugated anti-rabbit IgG (Molecular Probes) as the secondary antibody, were used. Briefly, the cultured cells were fixed in 4 % (vol/vol) paraformaldehyde (Wako Pure Chemical Industries, Ltd., Osaka, Japan) at room temperature for

15 min and treated with 50 mM glycine in phosphate-buffered saline (PBS) at room temperature for 30 min. The cells were treated with cold methanol at −20 °C for 15 min and permeabilized in PBS containing 0.2 % (vol/vol) Triton X-100 at room temperature for 15 min. Nonspecific binding was blocked with 1 % BSA in PBS at room temperature for 30 min. The fixed cells were incubated with the appropriate primary antibodies diluted in PBS containing 1 % BSA and 0.1 % Triton X-100 or Can Get Signal® immunostain solution A or B (Toyobo, Osaka, Japan) at 4 °C overnight. The rabbit polyclonal antibodies used as the primary antibodies were as follows: Golgi marker (giantin, sc-67168; Santa Cruz Biotechnology, Santa Cruz, CA), trans-Golgi network (TGN) markers including TGN46 (T7576; Sigma-Aldrich), TGN38 (sc-33783; Santa Cruz Biotechnology), syntaxin 6 (#2869; Cell Signaling technology, Beverly, MA) and TGOLN2, MVB marker (CD63, sc-15363; Santa Cruz Biotechnology), early endosomal marker (EEA1, E3906; sigma-aldrich), late endosomal marker (Rab7, sc-10767; Santa Cruz Biotechnology) and recycling endosomal marker (Rab11, #3539; Cell Signaling technology). After washing with PBS, the cells were stained with appropriate secondary antibodies diluted in PBS containing 1 % BSA and 0.1 % Triton X-100 or Can Get Signal® immunostain solution A or B (Toyobo) at room temperature for 2 h. The nuclei were counterstained with 4′,6-diamidino-2-phenylindole (DAPI; Roche Diagnostics, Mannheim, Germany). The slide glasses were mounted with Fluoromount/Plus (Diagnostic BioSystems, Pleasanton, CA) and then viewed under a FV1000 confocal laser microscope (Olympus, Tokyo, Japan). For the quantitation of co-localization in cells (mean ± standard error), at least 20 cells each were used for calculations in two independent experiments.

Expression of TGOLN2 recombinant protein

The expression plasmid for FLAG- and Myc-tagged TGOLN2 (pFLAG-Myc-CMV-22-TGOLN2) was constructed as follows. The coding sequence of TGOLN2 gene was amplified by PCR using a human cDNA clone of TGOLN2 (FCC138E05; Toyobo) as a template, *TaKaRa Ex Taq*® DNA polymerase (TaKaRa Bio, Otsu, Japan), and appropriate oligonucleotide primers. The sequences of the primers used were as follows: TGOLN2-EcoRI-A-335 P, 5′-TGAATTCAATGCGGTTCGTGGTTGCCTTGG-3′; *Eco*RI site (underlined) and plus-strand sequence (nt 335-356) of TGOLN2 gene, and TGOLN2-XbaI-1645 M, 5′-ATCTAGAGGACTTCTGGTCCAAACGTTGG-3′; *Xba*I site (underlined) and minus-strand sequence (nt 1624-1645) of TGOLN2 gene. The PCR product was subcloned into the T-vector pMD20 (TaKaRa Bio), and the nucleotide sequence between the *Eco*RI and *Xba*I sites of the derived clone was confirmed. The *Eco*RI-*Xba*I fragment of this subclone was ligated into pFLAG-Myc-CMV-22 (Sigma-Aldrich), from which the *Eco*RI-*Xba*I fragment had been removed, yielding pFLAG-Myc-CMV-22-TGOLN2.

PLC/PRF/5 cells in a four-well chamber slide (Nunc) were transfected with 0.5 μg of pFLAG-Myc-CMV-22-TGOLN2 using TransIT-LT1 reagent (Mirus Bio, Madison, WI) according to the manufacturer's recommendations. The empty vector was used as negative control. At 48 h after transfection, an immunofluorescence assay was performed to investigate the co-localization between the TGOLN2 recombinant protein and the antigen recognized by mAb TA1708, as described above.

Results

Production and characterization of mAbs

Six hybridoma clones secreting mAbs designated as TA1703, TA1705, TA1706, TA1707, TA1708 and TA1709 against the cell-culture-generated HEV particles were obtained in the present study. The specificity of these six mAbs was verified using immunocapture RT-PCR. Among them, mAb TA1708 (IgM class) exhibited the highest reactivity with viral particles associated with a membrane in the culture supernatant. Thereafter, mAb TA1708 was used in the further analyses. The membrane-associated HEV particles were efficiently captured by mAb TA1708 (86.8 %) (Table 1). In contrast, almost none of the viruses were captured by anti-ORF2 (H6225) or anti-ORF3 (TA0536) mAbs (5.3 % and 7.1 %, respectively). As with fecal HEV, no viruses were captured by mAb TA1708 (0.1 %). On the other hand, the viruses in feces that are known to be non-enveloped were efficiently trapped by the anti-ORF2 mAb (92.3 %) but not by the anti-ORF3 mAb (0.0 %). These results suggest that mAb TA1708 binds to membrane-associated HEV particles.

mAb TA1708 binds specifically to the membrane on the surface of HEV particles

To examine further whether mAb TA1708 binds to the membrane on the surface of viral particles, an immunocapture RT-PCR assay was performed using mAb TA1708, anti-ORF2 (H6225), and anti-ORF3 (TA0536) mAbs with or without prior treatment with detergents (Table 1). Consistent with our previous observations [39], when the particles in the culture supernatant were treated with 0.1 % or 1 % sodium deoxycholate, the efficiency of binding of HEV particles induced by anti-ORF2 mAb increased to 80.9 % and 84.2 %, respectively, while that induced by

Table 1 Reactivity of mAb TA1708 with HEV particles with or without prior treatment with detergents, as evaluated using immunocapture RT-PCR

Virus[a]	% of captured HEV in the total HEV per well		
	mAb TA1708	mAb H6225 (anti-ORF2)	mAb TA0536 (anti-ORF3)
Without pre-treatment with detergent			
Culture supernatant	86.8	5.3	7.1
Fecal supernatant	0.1	92.3	0.0
With pre-treatment with detergents[b]			
Culture supernatant			
0.1 % DOC-Na	14.6	80.9	59.0
1 % DOC-Na	11.2	84.2	44.3
0.1 % DOC-Na and 0.1 % trypsin	3.5	92.4	0.4
1 % DOC-Na and 0.1 % trypsin	0.8	94.1	0.2
0.1 % trypsin	73.5	7.1	0.2

[a] Viruses derived from the culture supernatant of infected cells (strain JE03-1760F) were subjected to immunocapture RT-PCR

[b] Prior to performing the immunocapture RT-PCR assay, the viruses were mixed with detergents, incubated at 37 °C for 2 hours, and then diluted 1:10 with PBS containing 0.1 % BSA

anti-ORF3 mAb increased to 59.0 % and 44.3 %, respectively. Furthermore, the binding efficiencies of HEV particles subjected to prior treatment with 0.1 % sodium deoxycholate and 0.1 % trypsin or 1 % sodium deoxycholate and 0.1 % trypsin increased to 92.4 % and 94.1 %, respectively, for the anti-ORF2 mAb and decreased to 0.4 % and 0.2 %, respectively, for the anti-ORF3 mAb. On the other hand, after treatment with these detergents or detergents/proteases, the binding efficiency of the viruses was reduced to 0.8-14.6 % for mAb TA1708 (Table 1). The virus particles in the culture supernatant treated with 0.1 % trypsin were efficiently captured by mAb TA1708 (73.5 %) but not by anti-ORF2 or anti-ORF3 mAbs (7.1 % and 0.2 %, respectively). These results indicate that mAb TA1708 binds specifically to a component of the membrane on the surface of HEV particles.

The membrane on the surface of HEV particles released into the culture supernatant is a lipid membrane

The HEV particles in the culture supernatant of the wild-type RNA- and ORF3-null mutant (ΔORF3) RNA-transfected cells were processed using digitonin, which effectively water-solubilizes lipids and has several membrane-related applications, including solubilizing membrane proteins and permeabilizing cell membranes, and changes in reactivity to mAb TA1708 were analyzed. After treatment with 1.5 % digitonin, the HEV particles were subjected to equilibrium centrifugation in a sucrose density gradient (Fig. 1). In agreement with the finding of our previous study [30], the wild-type HEV in the culture supernatant exhibited a peak density of 1.16 g/ml, while the ΔORF3 viruses in the culture supernatant banded at 1.27 g/ml in sucrose. The observed differences in buoyant density were found to be ascribable to the acquisition of the ORF3 protein and cellular membrane on the surface of the virions [38, 45]. The peak density of digitonin-treated virus particles in the culture supernatant of the wild-type RNA transfected cells shifted to 1.20 g/ml, a value that is between those observed for the membrane-associated HEV particles (1.16 g/ml) and the membrane-unassociated HEV particles (1.27 g/ml) (Fig. 1). On the other hand, the ΔORF3 mutant viruses in the culture supernatant banded at 1.27 g/ml, similar to fecal HEV, regardless of digitonin treatment.

To characterize the virus particles treated with digitonin that shifted to a peak density of 1.20 g/ml, an immunocapture RT-PCR assay was performed using anti-ORF2, ORF3 and TA1708 mAbs (Table 2). The membrane-associated particles (1.16 g/ml) in the culture supernatant of cells transfected with wild-type RNA were efficiently captured by mAb TA1708 (57.2 %), but not by the anti-

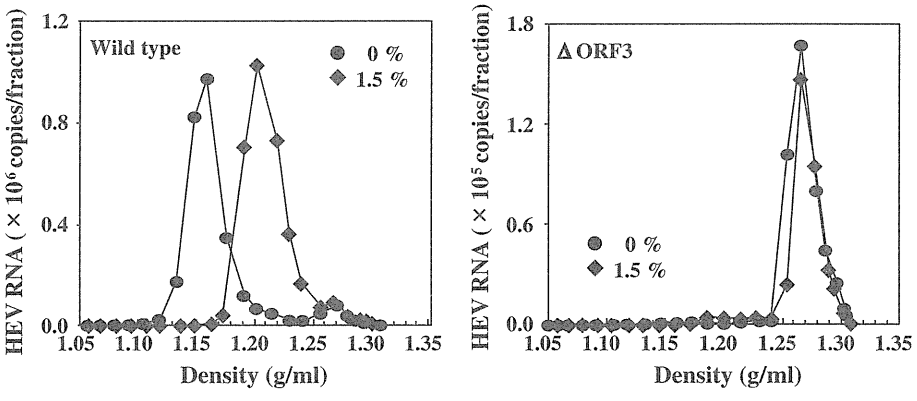

Fig. 1 Sucrose density gradient fractionation of HEV in the culture supernatants of RNA-transfected PLC/PRF/5 cells (wild-type and ΔORF3) with or without prior treatment with 1.5 % digitonin

Table 2 Reactivity of mAb TA1708 with membrane-associated and -unassociated HEV particles with or without prior treatment with 1.5% digitonin, as evaluated using immunocapture RT-PCR

Virus[a]	% of captured HEV in the total HEV per well		
	mAb TA1708	mAb H6225 (anti-ORF2)	mAb TA0536 (anti-ORF3)
pJE03-1760F/wt			
Without pre-treatment with digitonin (1.16 g/ml)	57.2	4.7	9.0
With pre-treatment with digitonin[b] (1.20 g/ml)	9.1	30.5	56.7
ΔORF3			
Without pre-treatment with digitonin (1.27 g/ml)	2.2	91.9	3.0
With pre-treatment with digitonin[b] (1.27 g/ml)	1.8	94.2	0.8

[a] Viruses were derived from the culture supernatants of transfected cells (pJE03-1760F/wt or ΔORF3) at 18 days post-transfection

[b] Prior to performing the sucrose density gradient centrifugation, the viruses were mixed with 1.5% digitonin and incubated at room temperature for 13 hours

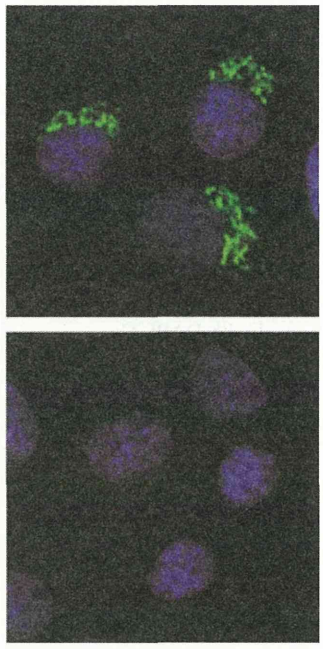

Fig. 2 Subcellular localization of the antigen recognized by mAb TA1708. PLC/PRF/5 cells were fixed and stained with mAb TA1708 and then labeled with Alexa Fluor 488–conjugated anti-mouse IgM. The nuclei were stained with DAPI. All images are representative of two independent experiments

ORF2 or anti-ORF3 mAb (4.7 % and 9.0 %, respectively). In contrast, the higher-density particles (1.20 g/ml) derived from digitonin treatment in the supernatant of the wild-type virus were trapped by both anti-ORF2 and anti-ORF3 mAbs (30.5 % and 56.7 %, respectively), while the efficiency of capture by mAb TA1708 was reduced to 9.1 % (Table 2). Viral particles with or without prior treatment with 1.5 % digitonin in the culture supernatant of the cells transfected with ΔORF3 RNA were efficiently captured by the anti-ORF2 mAb (94.2 % and 91.9 %, respectively), but not by the anti-ORF3 (0.8 % and 3.0 %, respectively) or TA1708 (1.8 % and 2.2 %, respectively) mAbs. These results indicate that the membrane on the surface of the viral particles generated in the culture supernatant is a lipid membrane.

Subcellular localization of the antigen recognized by mAb TA1708

We subsequently examined the subcellular localization of the antigen recognized by mAb TA1708 using immunofluorescence confocal microscopy. PLC/PRF/5 cells were prepared on a chamber slide and stained with mAb TA1708 and Alexa Fluor 488–conjugated anti-mouse IgM. Specific signals were observed only in the cytoplasm, primarily on the fringe and unevenly in the nucleus (Fig. 2, upper panel). In contrast, no specific signals were observed in the cells stained only with Alexa Fluor 488–conjugated anti-mouse IgM (Fig. 2, lower panel). These results indicate that mAb TA1708 reacts with intracellular antigens but not with the plasma membrane, suggesting that HEV forms membrane-associated particles in the cytoplasm, likely by utilizing the membranes of intracellular vesicles.

In order to identify the antigen recognized by mAb TA1708, we carried out double staining immunofluorescence assays using antibodies against well-established cellular markers (see Materials and methods). Although the antigen recognized by mAb TA1708 was co-localized with giantin and TGN46, strong co-localization was observed with TGN46 (Fig. 3). On the other hand, no clear co-localization was observed with the other cellular markers. Using anti-TGN38 and anti-syntaxin 6 antibodies, which are antibodies against TGN marker proteins, we performed double staining with mAb TA1708. The antigen recognized by mAb TA1708 exhibited a more distinct, pronounced co-localization signal between TGN38 and TGN46 when compared with syntaxin 6 (Fig. 4A). These results suggest that mAb TA1708 recognizes TGOLN2, which is encoded by the TGOLN2 gene and is also known as TGN38, TGN46, TGN48, TGN51 or TTGN2 [20, 25, 34]. Furthermore, we carried out double staining immunofluorescence studies using an anti-TGOLN2 antibody. The antigen recognized by mAb TA1708 also demonstrated co-localization in the double staining with TGOLN2 (Fig. 4B). These results suggest that TGOLN2 derived from TGN is a surface antigen of membrane-associated HEV particles.

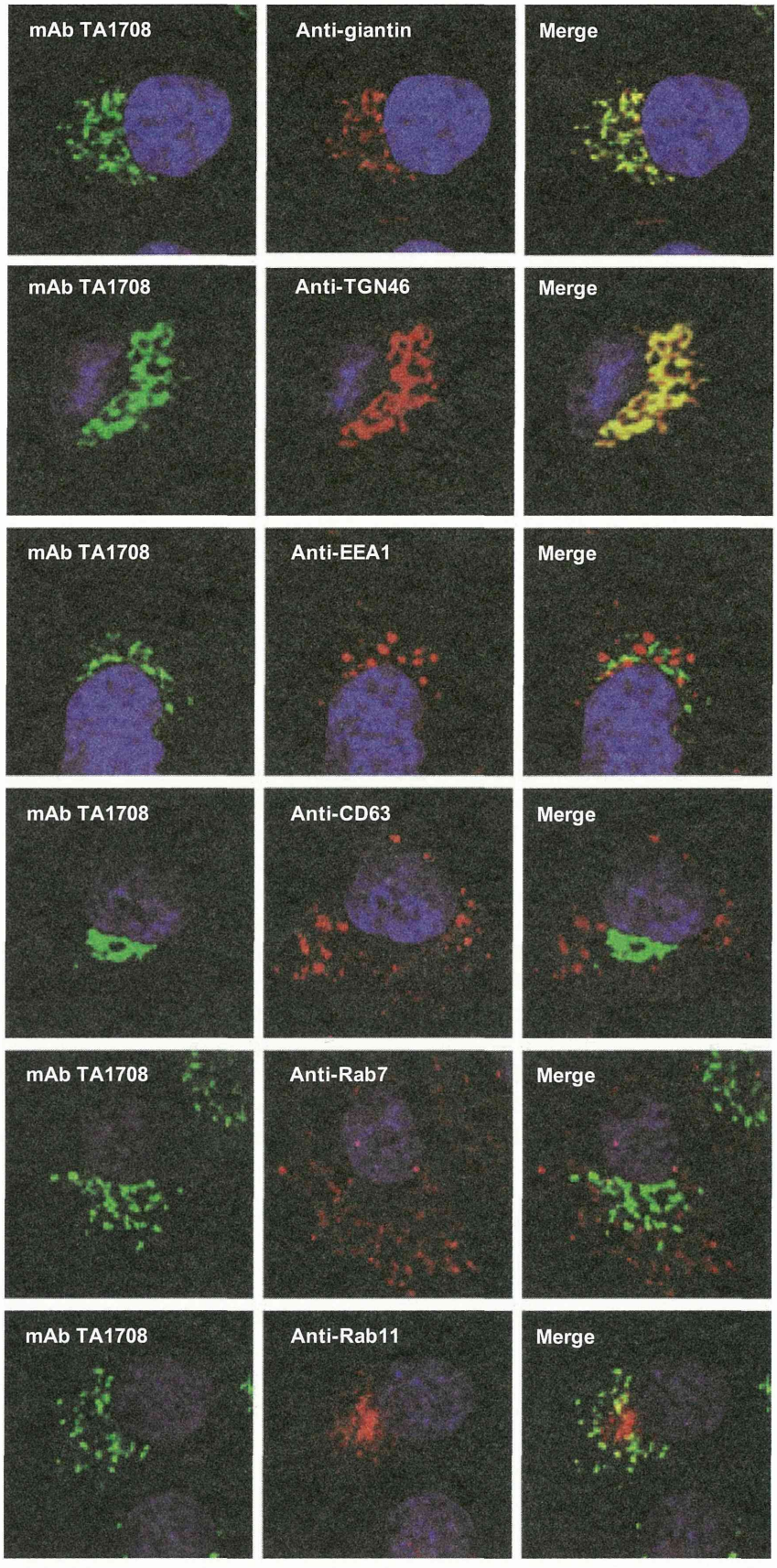

Fig. 3 Co-localization of the antigen recognized by mAb TA1708 with six established cellular markers. PLC/PRF/5 cells were fixed and double-stained with mAb TA1708 labeled with Alexa Fluor 488 and rabbit anti-giantin, anti-TGN46, anti-EEA1, anti-CD63, anti-Rab7, or anti-Rab11 antibodies labeled with Alexa Fluor 594. The nuclei were stained with DAPI. Co-localization is indicated by yellow staining. All images are representative of two independent experiments

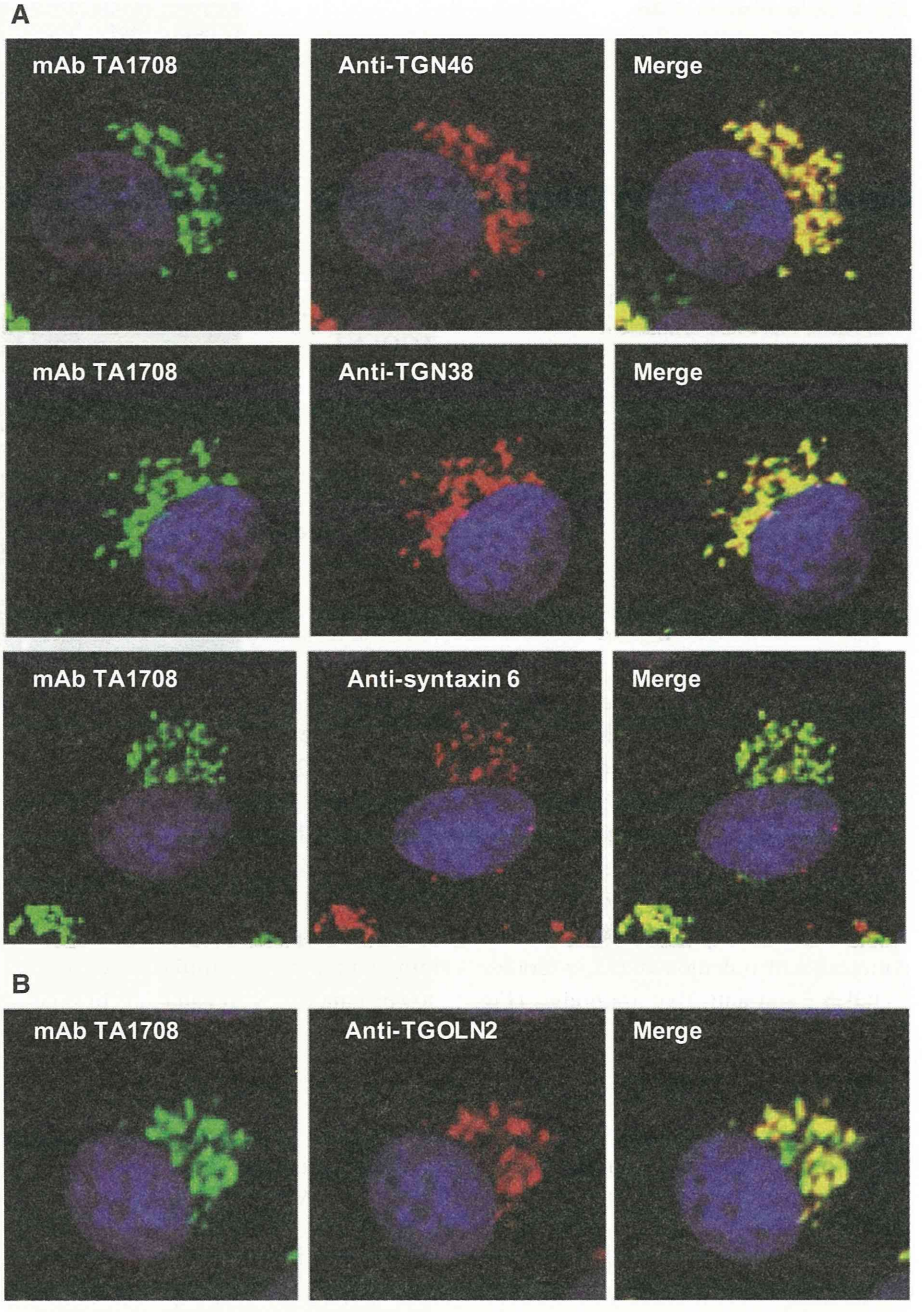

Fig. 4 Co-localization of the antigen recognized by mAb TA1708 with TGN markers. PLC/PRF/5 cells were fixed and double-stained with mAb TA1708 labeled with Alexa Fluor 488 and rabbit anti-TGN46, anti-TGN38, or anti-syntaxin 6 antibodies labeled with Alexa Fluor 594 (**A**) or rabbit anti-TGOLN2 antibodies labeled with Alexa Fluor 594 (**B**). The nuclei were stained with DAPI. Co-localization is indicated by yellow staining. All images are representative of two independent experiments

Intracellular localization of the expressed TGOLN2 recombinant protein and the antigen recognized by mAb TA1708

We subsequently examined the co-localization of Myc-tagged TGOLN2 protein and the antigen recognized by mAb TA1708 using immunofluorescence confocal microscopy. First, to confirm the specific detection of the Myc-tagged TGOLN2 expressed in the transfected cells, PLC/PRF/5 cells transfected with pFLAG-Myc-CMV-22-TGOLN2 or pFLAG-Myc-CMV-22 empty vector were stained with Alexa Fluor 488–conjugated anti-Myc mAb. The signal of Myc-tagged TGOLN2 stained by anti-Myc antibody was visible only in the cytoplasm, mainly on the nuclear periphery, of cells transfected with pFLAG-Myc-CMV-22-TGOLN2 (Fig. 5, middle-left panel), even though the specific signals of intracellular TGOLN2 were observed in the cytoplasm, primarily on the fringe and unevenly in the nucleus (Fig. 4B). In contrast, no specific signals were observed in the cells transfected with empty vector (Fig. 5, upper-left panel). These results indicate the specific detection of Myc-tagged TGOLN2 in the expressed cells by immunofluorescence assay using an anti-Myc antibody.

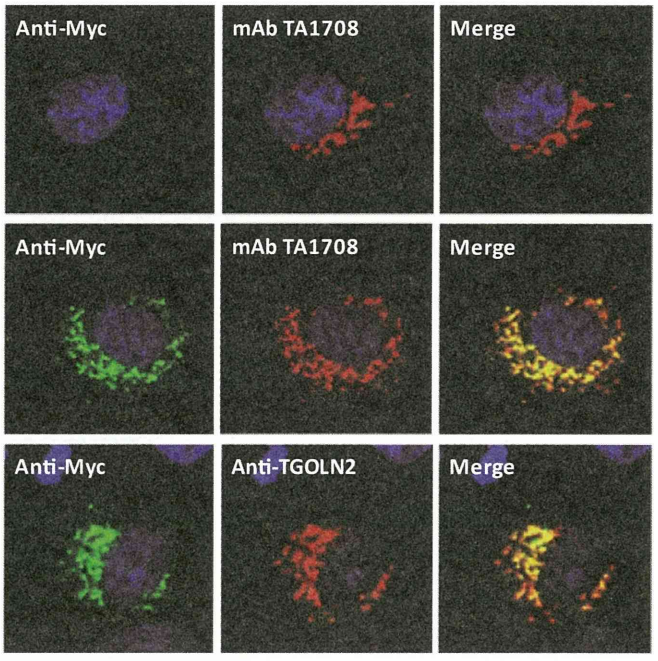

Fig. 5 Co-localization of the antigen recognized by mAb TA1708 with Myc-tagged TGOLN2 recombinant protein. PLC/PRF/5 cells were transfected with pFLAG-Myc-CMV-22 empty vector or pFLAG-Myc-CMV-22-TGOLN2. Cells were fixed and double-stained with anti-Myc mAb labeled with Alexa Fluor 488 and mAb TA1708 labeled with Alexa Fluor 568 or rabbit anti-TGOLN2 antibody labeled with Alexa Fluor 594. The nuclei were stained with DAPI. Co-localization is indicated by yellow staining. All images are representative of two independent experiments

To examine whether the antigen recognized by mAb TA1708 co-localizes with the expressed TGOLN2 protein, PLC/PRF/5 cells transfected with pFLAG-Myc-CMV-22-TGOLN2 were subjected to immunofluorescence assay. At least 20 different cells expressing Myc-tagged TGOLN2 were analysed in two independent experiments. A high degree of co-localization (97.5 ± 2.5 %) was observed in the cytoplasm (Fig. 5, middle panel). Similarly, co-localization was also demonstrated by double staining with anti-TGOLN2 and anti-Myc antibodies (Fig. 5, lower panel).

Membrane-associated HEV particles are generated intracellularly

In our previous study, an immunofluorescence assay using anti-ORF3 mAbs and antibodies against CD63, a MVB marker protein, revealed that ORF3 proteins are co-localized with CD63 in HEV-infected cells [31]. Furthermore, the mAb TA1708 against the membrane on the surface of HEV particles reacts with intracellular antigens (Fig. 2), thus suggesting that mature membrane-associated HEV particles are generated before being released from infected cells. To test our speculation that the membrane-associated virus particles are generated intracellularly, lysates of cells transfected with wild-type RNA were subjected to equilibrium centrifugation in a sucrose density gradient (Fig. 6). The viral particles in the cells transfected with the wild-type RNA exhibited a biphasic pattern, peaking at 1.15 and 1.26 g/ml, while the particles released into the culture supernatant banded in a single peak of 1.16 g/ml.

To characterize the cell-lysate-derived particles that were distributed into two major fractions, immunocapture RT-PCR was performed using TA1708, anti-ORF2 and anti-ORF3 mAbs, with or without prior treatment with 0.1 % sodium deoxycholate (Table 3). The higher-density particles (1.26 g/ml) in the cell lysates (fraction 3) of the cells transfected with wild-type RNA were efficiently captured by the anti-ORF2 mAb (81.5 %), but not by the TA1708 (0.0 %) or anti-ORF3 (0.8 %) mAbs, with or without prior treatment with 0.1 % sodium deoxycholate, similar to what was observed using the fecal supernatant (Table 1). In contrast, the lower-density particles (1.15 g/ml) derived from lysates of cells transfected with wild-type RNA (fraction 2) were captured by mAb TA1708 (46.0 %) without prior treatment with 0.1 % sodium deoxycholate as efficiently as the wild-type particles in the culture supernatant (fraction 1) (46.3 %). When the particles in fractions 1 and 2 were treated with 0.1 % sodium deoxycholate, the rate of capture by mAb TA1708 was reduced to 13.5 % and 13.9 %, respectively. On the other hand, the lower-density particles (fraction 2) were trapped by both anti-ORF2 and anti-ORF3 mAbs after treatment with 0.1 % sodium deoxycholate (64.3 % and 90.6 %, respectively), as efficiently as the wild-type particles in the culture supernatant (fraction 1) (62.2 % and 61.0 %, respectively). Furthermore, the viruses were not captured by anti-ORF2 or anti-ORF3 mAbs without treatment with 0.1 % sodium deoxycholate (11.6 % and 9.6 %, respectively), similar to the results obtained with the wild-type particles in the culture supernatant (9.5 % and 9.1 %, respectively) (Table 3). These results indicate that HEV particles with lipid membranes and ORF3 proteins on their surface are present abundantly in the lysates of cells transfected with wild-type HEV RNA.